

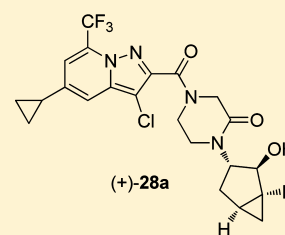
Hepatitis C Replication Inhibitors That Target the Viral NS4B Protein

John F. Miller, Pek Y. Chong, J. Brad Shotwell, John G. Catalano, Vincent W.-F. Tai, Jing Fang, Anna L. Banka, Christopher D. Roberts, Michael Youngman,[†] Huichang Zhang, Zhiping Xiong, Amanda Mathis,[‡] Jeffery J. Pouliot, Robert K. Hamatake, Daniel J. Price, John W. Seal, III, Lisa L. Stroup, Katrina L. Creech, Luz H. Carballo, Dan Todd, Andrew Spaltenstein, Sylvia Furst, Zhi Hong, and Andrew J. Peat*

GlaxoSmithKline Research and Development, 5 Moore Drive, Research Triangle Park, North Carolina 27709, United States

S Supporting Information

ABSTRACT: We describe the preclinical development and in vivo efficacy of a novel chemical series that inhibits hepatitis C virus replication via direct interaction with the viral nonstructural protein 4B (NS4B). Significant potency improvements were realized through isosteric modifications to our initial lead **1a**. The temptation to improve antiviral activity while compromising physicochemical properties was tempered by the judicious use of ligand efficiency indices during lead optimization. In this manner, compound **1a** was transformed into (+)-**28a** which possessed an improved antiviral profile with no increase in molecular weight and only a modest elevation in lipophilicity. Additionally, we employed a chimeric “humanized” mouse model of HCV infection to demonstrate for the first time that a small molecule with high in vitro affinity for NS4B can inhibit viral replication in vivo. This successful proof-of-concept study suggests that drugs targeting NS4B may represent a viable treatment option for curing HCV infection.

**INTRODUCTION**

Infection with hepatitis C virus (HCV) is well recognized as a global health issue that affects an estimated 170 million individuals.^{1,2} HCV is the leading cause of chronic hepatitis, liver cirrhosis, and hepatocellular carcinoma and accounts for approximately 350 000 deaths each year.^{3,4} The costs associated with HCV infection place tremendous burden on both the patients and the healthcare system as a whole.⁵ Currently, the standard of care (SoC) involves a combination of pegylated interferon (IFN), ribavirin, and one of two protease inhibitors recently approved by the FDA (telaprevir and boceprevir).^{6–8} Although the cure rates have improved dramatically, many patients cannot tolerate IFN and remain untreated.^{9,10} In addition, IFN is prohibitively expensive in many parts of the world; thus, there exists a high unmet need to develop IFN-free treatment regimens.

Tremendous progress has been made in the past decade in the development of direct acting antivirals (DAAs) for the treatment of HCV infection.^{11–15} The HCV genome encodes for three structural and seven nonstructural (NS) proteins,^{16–19} several of which have been targeted for pharmacological intervention. Compounds that directly inhibit the viral NS3/4A^{20–22} and NSSB^{22–24} enzymes, as well as compounds with an apparent NSSA²⁵ mechanism of action (MoA), have proven to be clinically effective in reducing viral replication and curing HCV infection. The discovery of drugs with varying MoAs enables combination therapy to combat viral resistance, analogous to the highly active antiretroviral therapy (HAART) used for the treatment of HIV.^{26,27} For the first time, drug cocktails containing oral DAAs show the potential to cure HCV infection and eliminate the need for IFN.^{28,29}

However, the error-prone nature of the HCV polymerase enzyme and the high rate of viral replication will likely necessitate the combination of at least two drugs with differing MoAs to provide effective treatment.³⁰

We recently reported^{31–33} on a novel series of substituted imidazo[1,2-*a*]pyridines that bind to the viral nonstructural protein 4B (NS4B).^{34–37} Importantly, a correlation between binding of NS4B and inhibition of HCV replication in vitro was observed for this chemical series.³¹ Our initial lead optimization effort yielded **1a** (Figure 1), a compound with high affinity for purified NS4B protein and low nanomolar activity against HCV genotype 1a and 1b replicons (Table 1).³¹ The antiviral potency and low dose pharmacokinetic (PK) profile in rat and dog supported further progression; however, escalating oral doses of **1a** in rats failed to achieve the higher plasma drug exposures required for preclinical safety studies. Furthermore, in vitro resistance passaging experiments employing wild-type HCV replicons revealed that single-point mutations within the NS4B protein render the virus partially resistant to **1a**.³¹ The ultimate impact of the resistance mutations on antiviral efficacy was difficult to predict given the lack of data pertaining to drugs that bind to NS4B. To date, no clinical or in vivo efficacy data have emerged to either validate NS4B as a viable target for treating HCV infection or assess the impact of resistance within a treatment paradigm.

Special Issue: HCV Therapies

Received: January 25, 2013

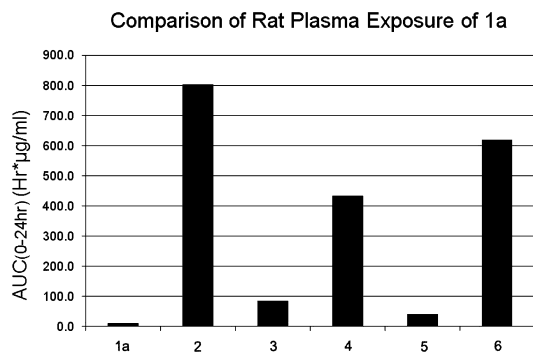
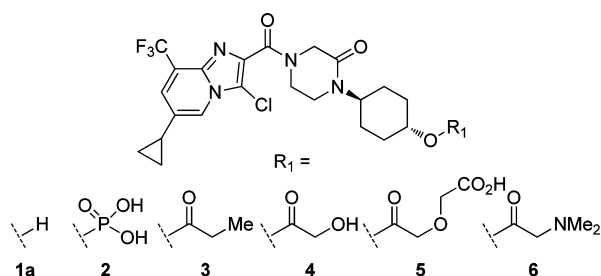


Figure 1. Plasma drug exposures of **1a** in rat following po administration of 300 mg/kg **1a** or prodrugs **2–6**.

Herein, we describe efforts to (1) improve the PK attributes of the lead molecule **1a** to support preclinical development, (2) demonstrate that small molecules interacting with NS4B can inhibit HCV replication in vivo, and (3) identify a new compound with an improved viral resistance profile relative to **1a**.

■ IN VIVO PROFILING OF THE LEAD **1A**

Evaluation of Prodrugs of 1a. The preclinical development of **1a** was contingent upon overcoming its inherently poor aqueous solubility (11 $\mu\text{g}/\text{mL}$ in FaSSiF) and obtaining higher plasma drug exposures. For example, a 300 mg/kg suspension dose of crystalline **1a**, wet-bead milled to maximize surface area for faster dissolution, resulted in relatively low exposure in rat ($\text{AUC} = 11.3 \mu\text{g}\cdot\text{h}/\text{mL}$, Figure 1). Alternative dosing formulations failed to achieve the desired outcome, and therefore, a prodrug strategy was devised. We selected two chemotypes (phosphate **2** and esters **3–6**, Figure 1) that are cleaved by different enzymes in vivo (phosphatases and esterases, respectively). For the esters, we also chose varying degrees of polarity and ionic character, from nonpolar (**3**) to polar (**4**) to acidic (**5**) to basic (**6**). The prodrugs **2–6** were dosed at 300 mg/kg (po) in rats, and the plasma concentrations of **1a** were determined. A side-by-side comparison found that the phosphate prodrug **2** delivered the highest plasma drug exposure of **1a** (Figure 1) which is likely due to its high FaSSiF solubility (>1000 $\mu\text{g}/\text{mL}$). Importantly, none of the phosphate prodrug itself (i.e., **2**) was detected in the blood of the rats, indicating rapid and efficient cleavage of the phosphate moiety by phosphatases present in the gut wall. In contrast, the esters gave lower plasma drug levels of **1a** and, in some cases, significant plasma concentrations of uncleaved prodrug. As an added benefit, the phosphate prodrug **2** formed a stable, crystalline solid that was easy to synthesize and therefore was selected for all forthcoming in vivo studies.

In Vivo PK and Efficacy of Prodrug 2 in PxB Mice. The species specificity of the hepatitis C virus has hindered the development of preclinical animal models of infection.³⁸ Chimpanzees are susceptible to HCV infection;³⁹ however, we chose to pursue a model involving chimeric “humanized” mice. The PxB mice are uPA/SCID mice with livers that have been repopulated with 70–90% human hepatocytes and, as a result, can be infected with human liver pathogens such as HCV and HBV.⁴⁰ We decided to use the PxB model to test whether an HCV antiviral agent that interacts with NS4B can inhibit viral replication in vivo.

Prodrug **2** was selected for use in the efficacy study, in part because of the high plasma drug exposures obtained in the rat PK studies. To ensure that the prodrug would also perform well in the efficacy model, the pharmacokinetic profile of **2** was determined in PxB mice ($n = 3/\text{group}$) prior to infection with HCV (Figure 2). Oral administration of **2** at doses of 10 and 30

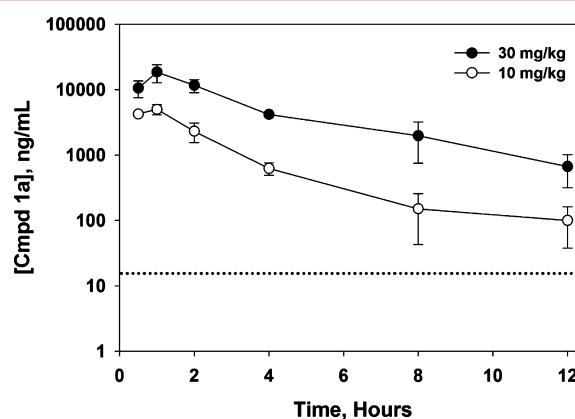


Figure 2. Plasma concentrations of **1a** over 12 h in PxB mice achieved upon po administration of prodrug **2** at 10 and 30 mg/kg. The dotted line represents the serum shifted EC_{90} (14 ng/mL) for **1a** versus the HCV genotype **1a** viral strain used to infect the mice.

mg/kg resulted in a linear increase in plasma drug exposures of **1a** ($\text{AUC}_{0-12\text{h}} = 15$ and $66 \mu\text{g}\cdot\text{h}/\text{mL}$, respectively). Both dose groups achieved 12 h plasma concentrations ($C_{12\text{h}}$) of **1a** well above the serum shifted EC_{90} of 29 nM (14 ng/mL) that was determined against the HCV genotype **1a** viral strain used to infect the PxB mice. We opted for b.i.d. dosing to ensure that the plasma drug levels of **1a** remained above the serum shifted EC_{90} throughout the 7-day study, thereby reducing the possibility for viral resistance that can occur with monotherapy treatment regimens. A repeat dose study with compound **2** was also conducted in PxB mice prior to infection to assess tolerability. The compound was well tolerated with no evidence of accumulation or induction of metabolism over 7 days of treatment (10 and 30 mg/kg b.i.d.). Furthermore, analysis of liver tissue 12 h after dosing on day 7 revealed modest (5- to 7-fold) partitioning of **1a** into the target organ (see Supporting Information).

PxB mice were infected with HCV genotype **1a** wild-type virus and after 5–8 weeks were treated with prodrug **2** ($n = 4/\text{group}$). Both the 10 and 30 mg/kg (b.i.d.) doses of prodrug **2** produced a rapid and robust drop (~ 1 log) in HCV viral mRNA titers (viral load) within 12 h of treatment (Figure 3). The maximum viral load reductions (~ 4 log units) occurred by day 4 for both dose groups; however, a dose-dependent decrease in viral load was apparent by day 7 (relative to baseline

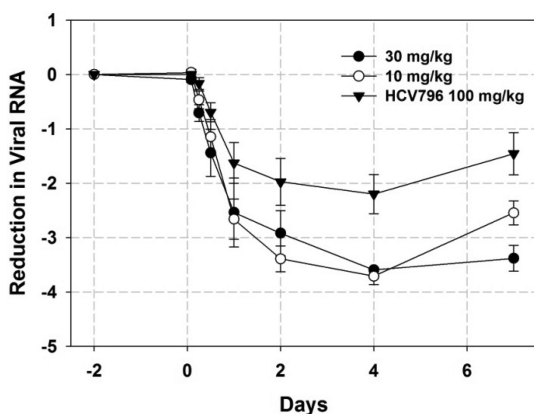


Figure 3. HCV viral RNA titers in PXB mice infected with HCV genotype 1a virus and treated for 7 days with prodrug **2** (10 or 30 mg/kg b.i.d.) or the positive control HCV-796 (100 mg/kg b.i.d.).

on day 0). The 30 mg/kg dose maintained viral suppression from day 4 through day 7, while the lower dose group (10 mg/kg) showed evidence of viral breakthrough at the end of the study. As a positive control, we included the non-nucleoside NSSB polymerase inhibitor HCV-796 which has demonstrated efficacy in human HCV clinical trials and in a HCV-infected chimeric mouse model similar to the one described here.⁴¹ In our study, all doses of prodrug **2** reduced HCV viral titers to a greater extent than did HCV-796, which was given at 100 mg/kg b.i.d. and produced a maximal viral load drop of ~2.2 log units (in good agreement with published results). A more detailed analysis of the data from this study, including the results from a 100 mg/kg b.i.d. dose group and the characterization of resistant viruses, is forthcoming.⁴² As far as we are aware, this represents the first in vivo proof of concept study associated with HCV inhibitors that bind to NS4B.

The high plasma exposure achieved with prodrug **2** also enabled the progression of **1a** into rat 7-day safety studies during which an adverse cardiovascular finding was identified that led to its termination. Encouraged by the robust antiviral response in the HCV mouse model, a backup effort was initiated to identify a replacement that would remove the cardiovascular risk and other limitations associated with **1a**. More specifically, we wanted to avoid the need for a prodrug and to improve upon the viral resistance profile, especially against the H94N and V105M mutated viruses found to be resistant to **1a**.³¹ A substantial number of compounds (>1500) in the imidazopyridine series had already been profiled as a result of our initial lead optimization effort, and therefore, we chose to pursue alternative chemical series.⁴³

■ IMPROVING POTENCY AGAINST RESISTANT VIRUSES

Identifying Alternative Core Scaffolds. Initially, we examined isosteric replacements of the imidazopyridine core and focused on new chemical series based on pyrazolopyridine **7**, benzimidazole **8**, and benzofuran **9** scaffolds (Figure 4). The syntheses of analogues **7a–9a** were undertaken to allow for a direct comparison to **1a**. The corresponding benzimidazole and benzofuran analogues (**8a** and **9a**, respectively) were synthesized in a straightforward manner (see Supporting Information). However, few reports existed for the preparation

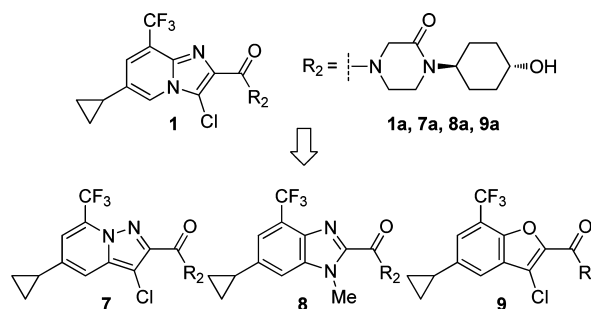
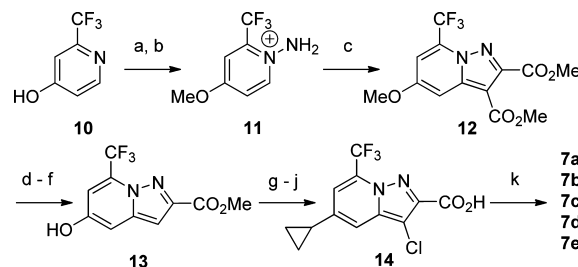


Figure 4. Structural modification of the initial NS4B compound **1a** led to analogues based on alternative scaffolds (**7a–9a**).

the 7- CF_3 -pyrazolo[1,5-*a*]pyridine derivatives, and therefore, we explored several synthetic routes toward this scaffold.

Syntheses of the Pyrazolo[1,5-*a*]pyridine Analogue (7a). The initial route to **7a** required the synthesis of carboxylic acid **14** and relied on the de novo construction of the pyrazolopyridine ring system (Scheme 1). Alkylation of

Scheme 1. Initial Route to the Pyrazolopyridine Acid **14** and Final Target Compounds **7a–e**^a



^aReagents and conditions: (a) MeI, K_2CO_3 , DMF (88%); (b) MSH, CH_2Cl_2 (62%); (c) DMAD, K_2CO_3 , DMF (49%); (d) H_2SO_4 , 90 °C; (e) AlBr_3 , EtSH; (f) H_2SO_4 , MeOH (73% over three steps); (g) $\text{PhN}(\text{Tf})_2$, DIPEA, CH_2Cl_2 (92%); (h) $\text{cPrB}(\text{OH})_2$, $\text{PdCl}_2(\text{dppf})$, CH_2Cl_2 , K_3PO_4 , 1,4-dioxane, 90 °C (84%); (i) NCS, DMF, 60 °C (94%); (j) 0.5 N NaOH, MeOH, 50 °C (quant); (k) for **7a**, 1-(*trans*-4-hydroxycyclohexyl)-2-piperazine hydrochloride, T3P, DIPEA, DMF (99%).

commercially available 2-(trifluoromethyl)pyridine-4-ol **10** with MeI afforded the corresponding methyl ether in high yield. N-Amination of the pyridine was problematic because of the low reactivity of the pyridyl nitrogen, a consequence of the electron-withdrawing *o*- CF_3 substituent. Ultimately, the use of a highly reactive N-aminating reagent, *O*-mesitylsulfonylhydroxylamine (MSH),^{44,45} was required to effect the desired transformation.⁴⁶ Intermediate **11** underwent a 1,3-dipolar cycloaddition reaction with dimethylacetylene dicarboxylate (DMAD) to give the pyrazolopyridine **12** in low-to-moderate yields.^{47,48} Heating **12** in the presence of H_2SO_4 led to ester hydrolysis followed by selective decarboxylation at C(3) of the pyrazolopyridine.⁴⁹ Cleavage of the methyl ether followed by Fischer esterification of the acid gave **13** in 73% yield for the three-step sequence.

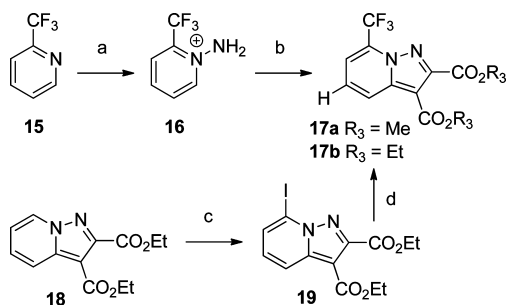
The remaining functional groups, cyclopropyl at C(5) and Cl at C(3), were installed in a straightforward manner (Scheme 1). Treatment of **13** with *N*-phenyltrifluoromethanesulfonamide gave the corresponding triflate, which underwent Pd-catalyzed cross-coupling with cyclopropylboronic acid in high yield. The addition of *N*-chlorosuccinimide followed by saponification of the ester gave the required pyrazolopyridine acid **14**, which was

coupled to the piperazinone amine fragment (**a**, Figure 4) to afford the final target compound **7a**.

The first-generation route (Scheme 1) provided gram quantities of the pyrazolopyridine acid **14** in 10 steps (14% overall yield) and was sufficient for establishing structure–activity relationships (SARs) within the new series. However, several synthetic issues needed to be addressed prior to the preparation of multigram batches required for *in vivo* studies. First, maintaining a reliable commercial supply of **10** proved to be capricious. In addition, the required protection/deprotection of the 4-hydroxyl group was inefficient. As our interest in the pyrazolopyridine scaffold increased during the course of lead optimization, an alternative route was sought to overcome these limitations.

A search for inexpensive starting materials that were reliably available in bulk from commercial vendors led us to 2-(trifluoromethyl)pyridine **15** as a key precursor. Treatment with MSH gave the *N*-aminated pyridine **16** that underwent 1,3-dipolar cycloaddition with DMAD to form **17a** in low yield (30%) for the two-step sequence (Scheme 2). Although

Scheme 2. Alternative Routes to 7-CF₃-pyrazolopyridine 17a,b Amenable to Large Scale Production^a



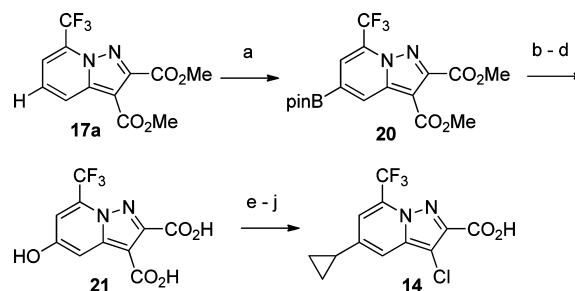
^aReagents and conditions: (a) MSH, CH₂Cl₂; (b) DMAD, K₂CO₃, DMF (30% over two steps); (c) 0.7 equiv of (TMP)₂Zn·2MgCl₂·2LiCl, THF, -10 °C, then I₂; (d) CuI, FSO₂CF₂CO₂Me, DMF, 80 °C (86% over two steps).

hundreds of grams of pyrazolopyridine **17a** were prepared by this method, the overall efficiency of the process was low. In addition, the large scale preparation of MSH was a safety concern due to the known thermal instability of the reagent.^{50,51} Seeking a safe and efficient route to kilogram quantities of **14**, we decided to avoid the *N*-amination/MSH reaction and begin with the pyrazolopyridine ring system already intact. No 7-(trifluoromethyl)pyrazolopyridine analogues were available from commercial vendors; however, the des-CF₃ analogue **18** could be purchased and represented an attractive starting point. After some optimization, we found that **18** could be efficiently converted to **17b** by a two-step procedure involving selective zincation/iodination at C(7)^{52,53} followed by Cu-mediated trifluoromethylation of the iodo intermediate **19** (Scheme 2).^{54,55} The zincation/iodination/trifluoromethylation procedure has been carried out successfully on 300 g of starting material **18**, which provided **17b** in 86% isolated yield.^{56,57}

With the 7-CF₃ group installed on the pyrazolopyridine core (**17a,b**), the introduction of functionality at C(5) was now required. Iridium-catalyzed activation of aromatic C–H bonds has proven to be a useful method for the functionalization of related aromatic ring systems.^{58–60} The selectivity of the reaction is dominated by steric effects and therefore appeared

well suited for substrate **17a,b**, as the C–H bond at C(5) is the least sterically hindered. In addition, we anticipated that the electron-deficient nature of the pyrazolopyridine ring system of **17a,b** would facilitate C–H bond activation. By employment of an Ir catalyst with bispinacolborane, the regioselective borylation of **17a** was accomplished in quantitative yield (Scheme 3). The boronate ester **20** could be isolated and

Scheme 3. Alternative Synthesis of 14 Based on Ir-Catalyzed C–H Activation^a



^aReagents and conditions: (a) [Ir(OMe)COD]₂, 4,4'-di-*t*-Bu-2,2'-bipyridine; (Bpin)₂, hexanes, 80 °C (quant); (b) H₂O₂; (c) Na₂SO₃; (d) aq NaOH (89%, four steps); (e) HCl, HOAc, 90 °C (76%); (f) MeOH, H₂SO₄ (quant); (g) Tf₂O, DIEA; (h) cPrB(OH)₂, Pd(OAc)₂, CataCXium A, K₃PO₄, toluene/water, 80 °C; (i) 1 M NaOH, then 1 M HCl (86%, three steps); (j) NCS, DCE, 50 °C (69%).

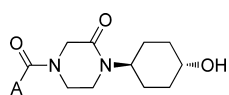
served as a versatile intermediate in Pd-catalyzed cross-coupling reactions. Alternatively, oxidation of the B–C bond afforded the phenol **21** that was converted to intermediate **14** in six steps.

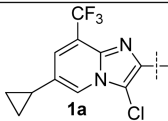
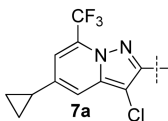
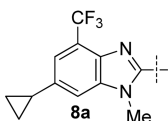
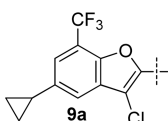
Examination of Alternative Core Series 7a–9a.

Analogues **7a–9a** were compared to **1a** in the NS4B binding and HCV replicon assays (Table 1). Substitution of the imidazopyridine core with other related bicyclic ring systems resulted in a modest improvement in binding affinity for NS4B protein. The pyrazolopyridine (**7a**) and benzofuran (**9a**) cores yielded the most significant gains in binding affinity, being about 4- to 13-fold more potent than the imidazopyridine (**1a**) core. The *N*-methylbenzimidazole (**8a**) scaffold was also well tolerated. The increase in binding affinity for NS4B (genotype 1b) protein directly translated to an increase in HCV (genotype 1b) replicon activity. For example, the pyrazolopyridine **7a** and benzofuran **9a** analogues were about 4-fold and 9-fold, respectively, more potent than **1a** in the genotype 1b replicon assay. Improvements of similar magnitude were also observed against the genotype 1a variant. No cellular toxicity was observed with these compounds following 2 days of treatment at 50 μM in Huh7 cells (see Supporting Information).

The antiviral activities of the modified core analogues **7a–9a** were also determined against stable NS4B-mutated replicons that were found to be resistant to **1a** (Table 1). In general, the increased activity in the binding assay was reflected in the resistant replicon assays. For example, the analogue with the highest affinity for NS4B (**9a**) was also the most active in the H94N and V105M replicon assays. Pyrazolopyridine **7a** also showed a significant improvement over **1a** against the H94N mutated replicon, while **8a** showed little difference.

Our effort to optimize antiviral activity was balanced with a desire to maintain the favorable physicochemical properties associated with **1a**. The increasing MW and lipophilicity of drug candidates over the past two decades are cited as underlying

Table 1. NS4B Binding Affinity and HCV Replicon Activity of Alternate Core Series (7a–9a)


A	Binding ^a		Replicon ^a		
	IC ₅₀ (nM)	1b	1a	1b	H94N
	53	1.0	7.0	200	730
	12	0.3	2.0	32	310
	24	0.5	3.0	150	230
	4	0.09	0.8	22	110

^aFor description of the assays and confidence intervals see Supporting Information and ref 31.

causes for late-stage attrition.⁶¹ To help reverse this trend, various drug efficiency indices have been developed,⁶² which allow chemists to relate structural modifications to changes in both the potency and the development risks associated with a molecule's physicochemical properties.⁶³ We utilized the lipophilic ligand efficiency (LLE)⁶⁴ index as a guide during lead optimization, as it emphasizes the development challenges associated with increasing lipophilicity even in the context of isosteric replacements. Although the use of calculated properties allows for prospective analysis and prioritization of target molecules, we prefer to assess the development risk of an existing asset based on experimentally determined measurements, in this case, a chromatographically measured log *D* designated below as ChromLogD (see Supporting Information).⁶⁵

The relative binding affinities and replicon potencies of core modifications 7a–9a were therefore considered in light of their impact on lipophilicity (ChromLogD, Table 2). While all three core replacements afforded improvements in binding affinity relative to 1a, the respective LLE_{meas} (=pIC_{50(NS4B Binding)} – ChromLogD) values of 7a–9a indicate that the benzimidazole 8a and benzofuran 9a represent less desirable structural changes relative to the pyrazolopyridine 7a in that their increased binding affinity was coupled with excessive increases in lipophilicity. For comparison, several other commonly considered drug efficiency indices are reported in Table 2, including binding efficiency index (BEI = (pIC₅₀/MW) × 1000) and lipophilic ligand efficiency determined using cLogP⁶⁶ (LLE_{calc} = pIC₅₀ – cLogP). The discrepant

Table 2. Physicochemical Properties and Drug Efficiency Indices for Analogues 1a and 7a–9a

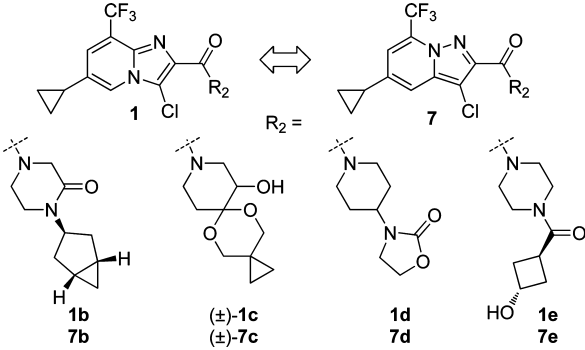
compd	MW	cLogP ^a (cLogD)	ChromLogD ^b	BEI	LLE _{calc}	LLE _{meas}
1a	485	3.1	3.5	15.1	4.2	3.8
7a	485	3.3	4.1	16.4	4.6	3.8
8a	464	2.7	4.3	16.4	4.9	3.3
9a	485	4.1	5.1	17.3	4.3	3.3

^aCalculated using the ACD/logD software described in ref 66.

^bNumber of replicates is ≥6. For description of the assay see Supporting Information and ref 65.

conclusions about the development risk associated with benzimidazole 8a and benzofuran 9a when using cLogP or MW as a surrogate for measured lipophilicity caution against the exclusive use of calculated values in guiding lead optimization decisions.

Comparison of Imidazo- versus Pyrazolopyridine Series. The low nanomolar activity of 7a against the H94N mutant replicon and its favorable physicochemical properties prompted further examination of the pyrazolopyridine core. Therefore, we combined acid 14 with several previously optimized amine tail fragments (b–e, Table 3) for which comparable imidazopyridine analogues had been made.^{31–33} Analysis of the matched molecular pairs revealed that in all cases, the pyrazolopyridine analogue was more potent than the

Table 3. NS4B Binding Affinity and HCV Replicon Activity for Matched Molecular Pairs 1/7b–e


compd	Binding ^a		Replicon ^a		
	IC ₅₀ (nM)	1b	1a	1b	H94N
1b	58	1.4	1.0	20	59
7b	4	0.1	0.06	0.7	2.0
(±)-1c	28	14	4.3	230	770
(±)-7c	10	4.0	1.9	39	250
1d	76	8.3	12	370	>1000
7d	37	2.0	5.0	94	370
1e	100	6.3	19	720	>1000
7e	42	2.0	8.3	330	>1000

^aFor description of the assays and confidence intervals see Supporting Information and ref 31.

corresponding imidazopyridine derivative with respect to NS4B binding (Table 3). On average, the pyrazolopyridine core enhanced binding affinity by 0.5 log units over the imidazopyridine scaffold. All of the tail fragments combined with the pyrazolopyridine core showed high affinity for NS4B protein ($IC_{50} < 40$ nM), including piperazinone **7b**, piperidinol **7c**, piperidine **7d**, and piperazine **7e**. A significant degree of structural diversity was tolerated at the peripheral end of the tail (compare **7c** with **7e**); however, the need for a hydrogen bond acceptor in the central portion of the tail became apparent. Optimal binding could be maintained with the H-bond acceptor positioned in either the central ring (examples **7b** and **7c**) or the terminal substituent (examples **7d** and **7e**).

As seen in the initial survey of core replacements (Table 1), the increased binding affinity of the pyrazolopyridine series translated to improved replicon activity (Table 3). For three of the four matched pairs (**1c–7c**, **1d–7d**, and **1e–7e**), the genotype 1b replicon activity of the pyrazolopyridine analogue improved 2- to 3-fold over the imidazopyridine counterpart, in line with the difference observed in the NS4B binding assay. A notable exception was the **1b–7b** pair, for which a 20-fold difference in replicon genotype 1b activity was observed between the two compounds with a 15-fold difference in binding affinity. The same trend was apparent in the H94N and V105M replicon assays. However, the low nanomolar binding activity ($IC_{50} = 4$ nM) for **7b** is at the upper limit of the assay (i.e., highest resolvable potency) and therefore may not be accurately determined, which could account for the apparent discrepancy between the binding and replicon activities. The exceptional replicon potency appeared unique to the [3.1.0]-bicyclohexane tail as analogue **7b** remains one of the most potent antiviral compounds we have seen within either chemical class.

Improving PK of Pyrazolopyridine Series. The antiviral activity of **7b** against the resistant replicons met our desired criteria, but the increased lipophilicity (ChromLogD = 6.4) was not optimal as reflected in the significantly eroded LLE_{meas} (2.0). In addition, compound **7b** exhibited high in vivo clearance in rats ($Cl = 70$ mL min^{-1} kg^{-1}). An analysis of the metabolites of **7b** generated in vitro from rat and human hepatocytes showed rapid oxidation of the terminal bicyclohexane substituent. We had found previously that the metabolism of an unsubstituted cyclohexane ring could be reduced by introducing a hydroxyl group, which ultimately led to **1a**.³¹ To determine if a similar tactic would improve the metabolic clearance of **7b**, a series of [3.1.0]bicyclohexanol analogues **22** were envisioned that required the preparation of amine fragments **23–25** (Figure 5). Initially, analogue **23** was deemed most attractive given the lack of stereogenic centers and

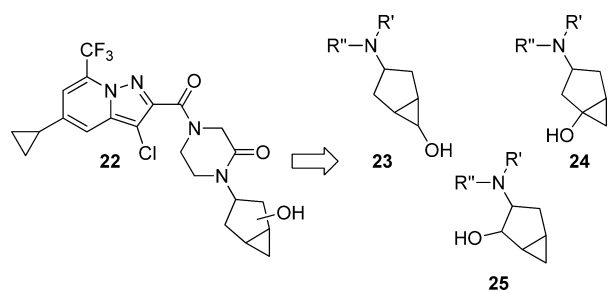


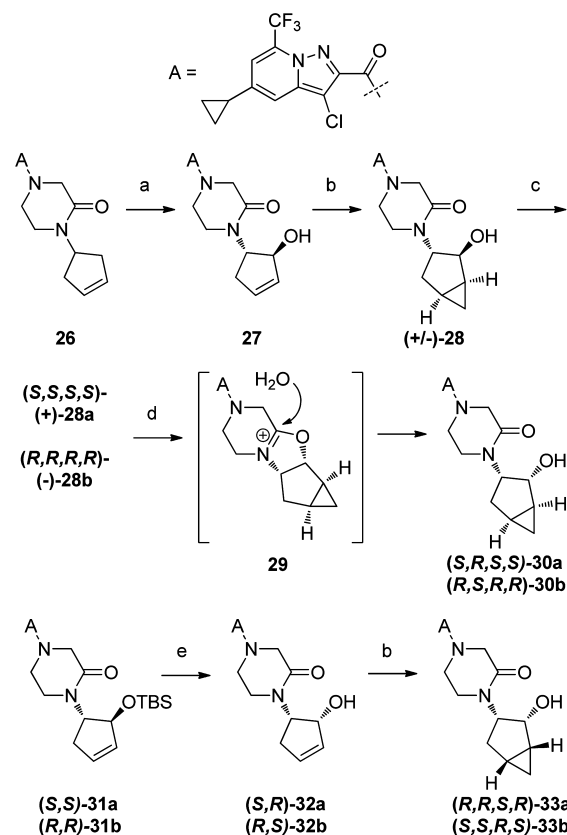
Figure 5. Envisioned [3.1.0]bicyclohexanol derivative **22** (and the requisite amine fragments **23–25**) designed to improve PK.

structural similarity with the 4-cyclohexanol derivatives known to bind NS4B (e.g., **1a** and **7a**). Unfortunately, the desired amine fragment appeared unstable under acidic conditions and further efforts were abandoned.⁶⁷ There were stability concerns and a lack of literature precedent related to amine fragment **24**, and therefore, attention shifted to the 2-hydroxybicyclohexanamines **25**.

Syntheses of [3.1.0]Bicyclohexan-2-ol Tail Analogues.

Allylic oxidation of the pendent cyclopentene ring of **26** occurred opposite the bulky piperazinone substituent, thereby affording **27** as a racemic mixture (Scheme 4).⁶⁸ The resulting

Scheme 4. Syntheses of [3.1.0]Bicyclohexan-2-ol Derivatives **28a/b**, **30a/b**, **33a/b**^a



^aReagents and conditions: (a) SeO_2 , 450:10:1 dioxane/water/pyridine, 105 °C (44%); (b) Et_2Zn , CH_2I_2 , DCM, 0 °C to rt (86% for **28**, 37% for **33a**); (c) chiral SFC chromatography; (d) 1:1 TFA/DCM, then water (90%); (e) 1:1 TFA/DCM, then 10% aq $NaHCO_3$ (quant).

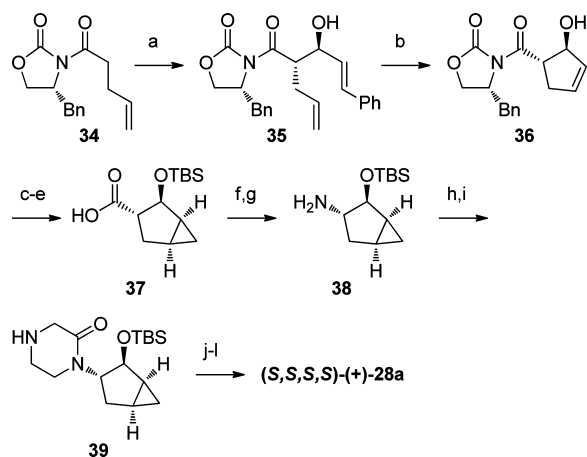
hydroxyl group directed the cyclopropanation to the *syn*-face of the olefin to give (\pm)-**28**,^{69,70} which upon resolution by chiral supercritical fluid chromatography (SFC) yielded enantiomers (+)-**28a** and (–)-**28b**. The relative stereochemistry was assigned by two-dimensional 1H NMR spectroscopy, and the absolute stereochemistry was confirmed as (*S,S,S,S*)-(+)-**28a** by single crystal X-ray crystallography (see Supporting Information).

While exploring the SAR within the [3.1.0]bicyclohex-2-ol series, we noted that treatment of (–)-**28b** with $POCl_3$ resulted in the efficient epimerization of the 2-hydroxyl group (Scheme 4). The inversion appears to occur via the cyclic intermediate **29**, which upon aqueous workup ring-opens to give the diastereomeric alcohol **30**. Other strong acids, such as TFA or

HCl, also promoted epimerization. By exploitation of this serendipitous finding, the enantiomerically pure alcohols (*S,R,S,S*)-**30a** and (*R,S,R,R*)-**30b** were prepared in high yield from analogues **28a** and **28b**, respectively. Taking further advantage of this pathway, we were able to access another diastereomer (**33**) by epimerizing the hydroxyl group before installing the cyclopropyl moiety. Treating the silyl-protected ether **31a** or **31b** with TFA, followed by addition of water, afforded the epimerized alcohol **32a** or **32b**, respectively. A hydroxyl-directed cyclopropanation using Et_2Zn and CH_2I_2 gave the desired enantiomers (*R,R,S,R*)-**33a** and (*S,S,R,S*)-**33b**, respectively. Ultimately, we were successful in preparing six of the eight possible stereoisomers (**28a/b**, **30a/b**, **33a/b**).

The low yield of the SeO_2 allylic oxidation and the need for chiral resolution of the resulting racemic mixture necessitated the development of a more efficient synthesis. By use of the Evans oxazolidinone, an asymmetric *anti*-aldol reaction between **34** and cinnamaldehyde installed two of the four desired stereocenters with a high diastereomeric ratio (19:1 dr) to give **35** (Scheme 5).⁷¹ Ring-closing metathesis of the diene **35** with

Scheme 5. Asymmetric Synthesis of (+)-**28a**^a



^aReagents and conditions: (a) *trans*-cinnamaldehyde, MgCl_2 , NaSbF_6 , TMSCl , TEA (88%); (b) third generation Grubbs catalyst, PhMe, rt (94%); (c) Et_2Zn , CH_2I_2 , DCM (89%); (d) TBSOTf, 2,6-lutidine, DCM (96%); (e) LiOH , H_2O_2 , THF/water (88%); (f) DPPA, TEA, PhMe, 80 °C; (g) KOTMS, THF (95% over two steps); (h) Ns-glycine, EDC, HOBT, DIPEA, DMF (quant); (i) 1,2-dibromoethane, Cs_2CO_3 , DMF, rt (82%); (j) PhSH, K_2CO_3 , MeCN (84%); (k) compound **14**, 50% T3P/EtOAc, DIPEA, THF, 0 °C to rt (quant); (l) TBAF, THF, 0 °C to rt (85%).

the third generation Grubb's catalyst afforded the cyclopentenol **36** in 94% yield. The hydroxyl-directed cyclopropanation of the olefin followed by protection of the alcohol and cleavage of the chiral auxiliary gave intermediate **37** as a single diastereomer in >95% enantiomeric excess. Curtius rearrangement of the carboxylic acid with DPPA and hydrolysis of the isocyanate with KOTMS afforded the amine **38** in 95% yield.⁷² The piperazinone was formed in two steps from **38** via amide formation with Nosyl-protected glycine followed by alkylation/ring closure with dibromoethane. Removal of the Nosyl group with thiophenol⁷³ gave **39**, which was subsequently coupled to the pyrazolopyridine acid **14**. Lastly, the silyl protecting group was removed with TBAF, thereby affording (+)-**28a** as a single isomer in >95% ee, the absolute stereochemistry of which was confirmed by single-crystal X-ray crystallography (see Support-

ing Information). The 11-step route (from **34**) provided access to >100 g of (+)-**28a** in 35% overall yield.

Comparison of the [3.1.0]bicyclohexanol Tail Analogues. All six of the [3.1.0]bicyclohexanol isomers displayed low nanomolar affinity for binding NS4B, which was predictive of the potent antiviral activity observed in the genotype 1b replicon assay (Table 4). Interestingly, much larger differences in activity were observed with the NS4B resistant replicons. For

Table 4. NS4B Binding Affinity and HCV Replicon Activity of [3.1.0]Bicyclohexan-2-ol Derivatives **28**, **30**, and **33**

	Binding ^a		Replicon ^a		
	IC ₅₀ (nM)		EC ₅₀ (nM)		
R ₃	1b	1a	1b	H94N	V105M
	4	0.1	0.06	0.7	2.0
	8	0.6	0.3	5.0	38
	23	4.0	2.3	38	65
	18	41	14	>1000	>1000
	18	7.9	4.9	64	400
	16	120	30	>1000	>1000
	23	95	19	>1000	>1000

^aFor description of the assays and confidence intervals see Supporting Information and ref 31.

example, isomers **30a**, **33a**, and **33b** were essentially inactive against the H94N and V105M resistant replicons while the (*S,S,S,S*) isomer [(+)-**28a**] exhibited low nanomolar activity. The (*R,R,R,R*)-(-)-**28b** also displayed good antiviral activity, although it was 5- to 7-fold less potent than its (+)-enantiomer. With respect to replicon activity, an *anti*-orientation of the 2-hydroxyl relative to the piperazinone ring appeared optimal (e.g., **28a/b**), whereas a *syn*-configuration was detrimental irrespective of the cyclopropane orientation (e.g., **30a/b** and **33a/b**).

The impact of these modifications on physicochemical properties was also examined and compared to **1a** (Table 5).

Table 5. Physicochemical Properties and Drug Efficiency Indices for Analogues **1a, **7b**, and (+)-**28a****

compd	MW	cLogP ^a (cLogD)	Chrom- LogD ^b	BEI	LLE _{calc}	LLE _{meas}
1a	485	3.1	3.5	15.1	4.2	3.8
7b	467	4.0	6.4	18.0	4.4	2.0
(+)- 28a	483	2.8	4.6	16.8	5.3	3.5

^aCalculated using the ACD/logD software described in ref 66.

^bNumber of replicates is ≥ 6 . For description of the assay see Supporting Information and ref 65.

Introduction of the 2-hydroxyl in (+)-**28a** dramatically improved the measured lipophilicity relative to **7b** (Chrom-LogD = 4.6 versus 6.4, respectively). When compared to **1a**, (+)-**28a** shows a significant increase in the measured log *D*; however, the increase in lipophilicity appears roughly commensurate with the increase in binding affinity, as the LLE_{meas} values are comparable (3.8 and 3.5 for **1a** and **28a**, respectively). The impact of the increased lipophilicity of (+)-**28a** relative to **1a** is not negligible, however, and was reflected in an overall greater binding to plasma proteins across species (Table 6). The degree of plasma protein binding

Table 6. Plasma Protein Binding (%) Across Species for **1a and (+)-**28a**^a**

compd	human	monkey	dog	rat	mouse
1a	83	77	66	80	ND
(+)- 28a	94	91	93	96	97

^aFor description of the assay see Supporting Information.

observed for (+)-**28a** is still considered moderate when compared to many drug candidates. Ironically, there was a 30-fold improvement in the FaSSIF solubility of (+)-**28a** relative to **1a** (0.31 versus 0.011 mg/mL) despite the increased lipophilicity.

Efficiency indices based on calculated values are also presented for comparison (BEI and LLE_{calc}). As seen previously, the efficiency values derived from MW and calculated log *P/D* values may underestimate the risks associated with developing a compound such as **7b** and should be interpreted with caution.

Pharmacokinetic Profile of (+)-28a**.** The initial justification for pursuing the complex chiral tail of (+)-**28a** was the hypothesis that introducing a hydroxyl group would improve metabolic stability. Therefore, the in vitro metabolism of (+)-**28a** was examined in hepatocytes from five species.^{74,75} Consistent with the findings in the cyclohexane series, adding the 2-hydroxyl substituent (**28a**) resulted in a lower predicted

clearance relative to the unsubstituted bicyclohexane (**7b**) derivative across all species (Table 7). The effect was most

Table 7. In Vitro Predicted Clearance^a of **7b and (+)-**28a****

compd	human	monkey	dog	rat	mouse
7b	18	34	30	41	80
(+)- 28a	<5	11	<5	24	<5

^aClearance units (mL min⁻¹ kg⁻¹). For description of the assay see Supporting Information.

pronounced in human, dog, and mouse hepatocytes, in which (+)-**28a** appeared most stable. A more modest improvement (2- to 3-fold) was seen in rat and monkey hepatocytes. Separate in vitro studies showed that (+)-**28a** did not inhibit cytochrome P450 isozymes (IC₅₀ > 20 μM versus 3A4, 1A2, 2C9, 2C19, 2D6) or generate reactive metabolites in a glutathione-trapping assay (rat and human microsomes).

The improved in vitro metabolic stability of (+)-**28a** versus **7b** translated to reduced clearance in vivo (Table 8). For

Table 8. In Vivo Pharmacokinetic Profiles of (+)-28a**^f**

species	iv ^a			po ^b	
	Cl (mL min ⁻¹ kg ⁻¹)	Vd _{ss} (L/kg)	t _{1/2} (h)	AUC _{0-∞} (μg·h/mL)	F (%)
mouse ^c	19	0.6	0.4	1.0	12
rat ^d	25	2.0	2.0	3.1	92
dog ^e	6.0	0.7	2.0	25	>100
cyno ^e	3.0	0.7	4.0	25	97

^aDosed iv at 1 mg/kg in DMSO/20% HP-β-CD (10:90). ^bDosed orally at 5 mg/kg in DMSO/20% HP-β-CD (10:90). ^civ (*n* = 4); po (*n* = 4). ^div (*n* = 3); po (*n* = 2). ^eiv (*n* = 3); po (*n* = 3). ^fFurther details available in Supporting Information.

example, the rat clearance of (+)-**28a** was 3-fold lower than that of **7b** (25 versus 70 mL min⁻¹ kg⁻¹, respectively), which correlated with the 2-fold improvement in predicted clearance observed in rat hepatocyte studies. Overall, (+)-**28a** displayed low-to-moderate clearance across four species and >90% bioavailability in all species except mouse. High plasma drug exposures were also achieved with low doses (5 mg/kg) in both dog and monkey. The improved pharmacokinetic profile coupled with the favorable FaSSIF solubility resulted in increased plasma exposure upon escalation of dose that enabled progression to 7-day safety studies without the need for a prodrug.

CONCLUSION

For the first time, a small molecule that inhibits HCV replication via an apparent NS4B mechanism of action has demonstrated in vivo efficacy in a chimeric “humanized” mouse model of HCV infection. Over a 7-day course of treatment, a prodrug of compound **1a** produced rapid and dose-dependent decreases in HCV serum RNA that surpassed that of a clinically validated positive control, HCV-796. The successful proof-of-concept study indicates that drugs targeting NS4B may represent viable treatment options for curing HCV infection that could further expand combination regimens.

Our efforts to optimize antiviral potency while maintaining favorable physicochemical properties prompted us to examine isosteric analogues of our lead **1a**. Replacement of the imidazopyridine core with an analogous pyrazolopyridine

scaffold yielded a modest, but consistent, increase in both NS4B binding affinity and antiviral activity against HCV replicons. More significant improvements were realized with isosteric modifications in the amide (tail) portion of the series, whereby bridging the terminal cyclohexyl substituent to form a [3.1.0]bicyclohexane ring afforded an analogue with $IC_{50} < 1$ nM in the replicon assays. The temptation to improve antiviral activity at the cost of increased MW or lipophilicity was tempered by the judicious use of efficiency indices such as BEI and LLE during lead optimization. However, a direct consequence of this approach was the need to construct densely functionalized fragments as exemplified by a unique chiral 2-bicyclohexanolamine. In this manner, the original lead **1a** was transformed into (+)-**28a** which possessed an improved antiviral profile against the resistant NS4B-mutated replicons and low nanomolar activity against HCV genotypes 3a, 4a, and 5a.⁴³ Compound (+)-**28a** had no increase in molecular weight and only a modest elevation in lipophilicity relative to **1a**, which manifested in improved FaSSIF solubility and PK. The need for a prodrug was thereby eliminated, and (+)-**28a** progressed into 7-day preclinical safety studies, the results of which will be published in due course.

EXPERIMENTAL SECTION

All commercially obtained solvents and reagents were used as received. The purity of the final compounds was determined to be $\geq 95\%$ by ¹H NMR and LCMS; structural assignments were consistent with the spectroscopic data. ¹H NMR spectra were taken on a Varian (Agilent) Inova 400 NMR spectrometer. Chemical shifts are reported in parts per million (ppm, δ) using the residual solvent line as a reference. Splitting patterns are designated using the following abbreviations: s, singlet; d, doublet; t, triplet; dd, doublet of doublet; m, multiplet; br, broad. Coupling constants (*J*) are reported in hertz (Hz). Mass spectrometric analyses and compound purity determinations were conducted on a Waters Acquity UPLC system (Phenomenex Kinetex column at 40 °C, mobile phase of water with 0.2% v/v formic acid and acetonitrile with 0.15% v/v formic acid) and Waters Acquity SQD with alternating positive/negative electrospray ionization scanning from 125 to 1000 amu, with a scan time of 105 ms and an interscan delay of 20 ms. High resolution mass spectrometric analysis was performed on a Waters qTOF Premiere mass spectrometer using flow injection operating in W mode. Chiral analytical HPLC was performed on an Agilent 1100 analytical system. Optical rotations were measured using a Rudolph Research Analytical Autopol V polarimeter.

1-Amino-2-(trifluoromethyl)pyridinium 2,4,6-Trimethylbenzenesulfonate (16). A solution of 2-(trifluoromethyl)pyridine (10.0 g, 68.0 mmol) and *O*-mesitylenesulfonylhydroxylamine (19.0 g, 88.0 mmol; see Mendiola et al. *Org. Process Res. Dev.* **2009**, *13*, 263) in DCM (170 mL) was stirred at room temperature for 4 days, at which point the reaction was still incomplete. An additional portion (7.3 g, 34 mmol) of *O*-mesitylenesulfonylhydroxylamine was added, and the reaction mixture was stirred for another day. No further progress was observed by NMR. The reaction mixture was evaporated to dryness to afford crude **16** which was used without further purification. ¹H NMR (400 MHz, DMSO-*d*₆): δ 9.19 (d, *J* = 6.1 Hz, 1 H) 8.64–8.73 (m, 1 H) 8.58–8.64 (m, 1 H) 8.34–8.42 (m, 1 H) 8.26 (s, 2 H) 2.17 (s, 9 H).

Dimethyl 7-(Trifluoromethyl)pyrazolo[1,5-*a*]pyridine-2,3-dicarboxylate (17a). Dimethyl acetylenedicarboxylate (16.8 mL, 136 mmol) was added by dropwise addition to a 0 °C solution of **16** (crude mixture from previous step, 68 mmol theoretical) and potassium carbonate (18.8 g, 136 mmol) in DMF (170 mL). Air was bubbled through the reaction mixture for a few minutes, and stirring was continued at room temperature overnight. Water (400 mL) was added, and the solution was stirred for 30 min. The resulting solid was collected by vacuum filtration, washed with water, dried, and purified by flash chromatography (silica gel, 25–33% EtOAc/hexane)

to afford **17a** (6.2 g, 30% over two steps) as a tan solid. ¹H NMR (400 MHz, DMSO-*d*₆): δ 8.40 (d, *J* = 8.8 Hz, 1 H) 7.91 (d, *J* = 6.6 Hz, 1 H) 7.77–7.84 (m, 1 H) 3.95 (s, 3 H), 3.87 (s, 3 H). ES-LCMS *m/z*: 303 (*M* + 1).

5-Hydroxy-7-(trifluoromethyl)pyrazolo[1,5-*a*]pyridine-2,3-dicarboxylic Acid (21). A solution of **17a** (40.0 g, 0.134 mol), [Ir(OMe)COD]₂ (2.63 g, 3.97 mmol), 4,4'-di-*tert*-butyl-2,2'-bipyridine (2.06 g, 7.70 mmol), and bis(pinacolato)diboron (33.6 g, 132 mmol) in degassed cyclopentyl methyl ether (320 mL) was heated to 80 °C for 1.3 h. The mixture was allowed to cool to room temperature and immersed in an ice bath. To the mixture was slowly added 30% aqueous hydrogen peroxide (27 mL, 625 mmol) while keeping the temperature at or below 25 °C. After 2 h, 15% aqueous sodium bisulfite (222 mL) was added, keeping the temperature under 10 °C. The reaction mixture was left overnight, cooled to 0 °C, and filtered. The filtrate phases were separated, and the organic phase was isolated. A solution of 50% aqueous NaOH (37 g) diluted to 232 mL with water was added. The solution was heated to 80 °C for 2 h. The solution was cooled to room temperature, and the phases were separated. The aqueous phase was cooled to 5 °C. HCl (5 equiv) was added and the mixture held at room temperature overnight. The suspension was cooled to 5 °C and the solid collected by filtration. The solid was washed with water and dried at reduced pressure at 60 °C overnight to afford **21** (34 g, 89%). ¹H NMR (400 MHz, DMSO-*d*₆): δ 11.28 (s, 1H), 7.83 (s, 1H), 7.30 (s, 1H).

3-Chloro-5-cyclopropyl-7-(trifluoromethyl)pyrazolo[1,5-*a*]pyridine-2-carboxylic Acid (14). (A) **5-Hydroxy-7-(trifluoromethyl)pyrazolo[1,5-*a*]pyridine-2-carboxylic Acid.** Compound **21** (388 g, 1.34 mol) was added to a reactor along with AcOH (1552 mL, 27.10 mol) and 12 M aqueous HCl (217 mL, 2.60 mol). The mixture was heated to 90 °C and stirred until the reaction was determined to be complete by HPLC (4 h). The mixture was cooled to 20 °C, and water (3880 mL) was added to the reactor. The suspension was then cooled to 10 °C and stirred overnight. The resulting solid was collected by filtration, washed with water, and dried under vacuum at 50 °C for 3 days to afford the title compound (248 g, 76%). ¹H NMR (400 MHz, DMSO-*d*₆): δ 13.20 (br s, 1 H), 10.91 (s, 1 H), 7.24 (d, *J* = 2.3 Hz, 1 H), 7.18 (d, *J* = 2.3 Hz, 1 H), 6.95 (s, 1 H). ES-LCMS *m/z*: 245 (*M* - 1).

(B) **Methyl 5-Hydroxy-7-(trifluoromethyl)pyrazolo[1,5-*a*]pyridine-2-carboxylate (13).** 5-Hydroxy-7-(trifluoromethyl)pyrazolo[1,5-*a*]pyridine-2-carboxylic acid (0.260 g, 1.06 mmol) was dissolved in MeOH (5 mL), and concentrated sulfuric acid (3 drops) was added. The solution was heated under reflux for 1.5 h. Water was added, and the mixture was extracted with EtOAc. The organic phase was dried over sodium sulfate and the solvent evaporated to afford **13** as a light yellow solid (0.28 g, quant). ¹H NMR (400 MHz, methanol-*d*₄) δ ppm 7.16 (d, *J* = 2.4 Hz, 1 H), 7.09 (d, *J* = 2.3 Hz, 1 H), 6.95 (s, 1 H), 3.95 (s, 3 H). ES-LCMS *m/z*: 261 (*M* + 1).

(C) **5-Cyclopropyl-7-(trifluoromethyl)pyrazolo[1,5-*a*]pyridine-2-carboxylic Acid.** DIPEA (176 mL, 1.01 mol) was added to a solution of **13** (105 g, 0.400 mol) in DCM (1.05 L). The solution was cooled to 0 °C, and triflic anhydride (75 mL, 0.44 mol) was added at a rate to maintain the temperature below 10 °C. Once the reaction was determined to be complete by HPLC, 13% aqueous sodium chloride was added and the solution was stirred for 20 min. Stirring was stopped, and the layers were separated. The upper aqueous layer was removed. The organic layer was distilled to 1/3 volume, and toluene (1.1 L) was added. Cyclopropylboronic acid (69.2 g, 0.810 mol), CataCXium A (3.61 g, 10.0 mmol), potassium phosphate tribasic (258 g, 1.21 mol), and water (474 mL) were then added. Lastly, palladium acetate (2.26 g, 10.0 mmol) was added and the mixture was heated to 80 °C. The reaction was monitored by HPLC until complete, and then the mixture was cooled to 25 °C. With stirring, additional water (316 mL) was added, and after 10 min the layers were allowed to separate. The lower aqueous layer was removed and discarded. The organic layer was diluted with THF (316 mL) and 1 N aqueous NaOH (1106 mL) and heated to 50 °C. When the saponification was determined to be complete by HPLC, the mixture was cooled to 25 °C and the layers were allowed to separate. The bottom aqueous layer was isolated and

acidified using 1 N aqueous HCl (1185 mL) and cooled to 10 °C. The resulting solid was collected by filtration, washed with water, and dried under vacuum at 50 °C to give the title compound (86 g, 86%).

(D) **3-Chloro-5-cyclopropyl-7-(trifluoromethyl)pyrazolo[1,5-*a*]pyridine-2-carboxylic Acid (14)**. A mixture of 5-cyclopropyl-7-(trifluoromethyl)pyrazolo[1,5-*a*]pyridine-2-carboxylic acid (100 g, 0.370 mol) in 1 L of DCE was heated at reflux and 200 mL of DCE removed by distillation to ensure dryness of the substrate. The solution was cooled to 25 °C. *N*-Chlorosuccinimide (73 g, 0.46 mol) was added to the reactor, and the solution was heated at 50 °C. When the reaction was complete by HPLC, the mixture was cooled to 25 °C, and 1 M aqueous NaOH (1 L) was added. The mixture was stirred for 2 h, and the layers were separated. While stirring, the aqueous layer was acidified to pH 1 with 6 M aqueous HCl. The suspension was stirred and cooled to 10 °C. The solid was collected by filtration, washed with water (500 mL), and dried under vacuum at 50 °C to constant weight to afford **14** (78 g, 69%) as a white solid. ¹H NMR (400 MHz, DMSO-*d*₆): δ 13.70 (br s, 1 H), 7.71 (s, 1 H), 7.47 (br s, 1 H), 2.17–2.29 (m, 1 H), 1.05–1.14 (m, 2 H), 0.94–1.03 (m, 2 H). ES-LCMS *m/z*: 305 (M + 1).

Asymmetric Synthesis of 4-[[3-Chloro-5-cyclopropyl-7-(trifluoromethyl)pyrazolo[1,5-*a*]pyridin-2-yl]carbonyl]-1-[(1*S*,2*S*,3*S*,5*S*)-2-hydroxybicyclo[3.1.0]hex-3-yl]-2-piperazine (28a). (A) **(4*R*)-3-(4-Pentenoyl)-4-(phenylmethyl)-1,3-oxazolidin-2-one (34)**. To a solution of **(4*R*)-4-(phenylmethyl)-1,3-oxazolidin-2-one** (2.50 g, 14.0 mmol) in THF (40 mL) under nitrogen at –78 °C was added dropwise 1.6 M *n*-BuLi in hexane (9.17 mL, 14.7 mmol), and the resulting mixture was stirred at –78 °C for 1 h. Then a solution of 4-pentenoyl chloride (1.60 mL, 14.1 mmol) in THF (10 mL) was added dropwise. After being stirred at –78 °C for 1 h, the reaction mixture was allowed to warm to room temperature and stirred overnight. After being diluted with water, the mixture was extracted with EtOAc (2 × 60 mL). The combined EtOAc extracts were washed with brine, dried over sodium sulfate, filtered, and concentrated to dryness at reduced pressure. The crude residue was purified by flash chromatography (silica gel, 0–20% EtOAc/hexane) to give **34** (3.29 g, 91%) as a light yellow oil. ¹H NMR (400 MHz, CDCl₃): δ 7.25–7.39 (m, 3 H), 7.20–7.23 (m, 2 H), 5.82–5.95 (m, 1 H), 5.12 (dd, 1 H, *J* = 17.1 Hz, 1.7 Hz, 1 H), 5.05 (dd, *J* = 10.1 Hz, 1.2 Hz, 1 H), 4.65–4.74 (m, 1 H), 4.15–4.25 (m, 2 H), 3.31 (dd, *J* = 13.3 Hz, 3.3 Hz, 1 H), 2.96–3.18 (m, 2 H), 2.76 (dd, *J* = 13.3 Hz, 9.6 Hz, 1 H), 2.42–2.54 (m, 2 H).

(B) **(4*R*)-3-[(2*S*,3*S*,4*E*)-3-Hydroxy-5-phenyl-2-(2-propen-1-yl)-4-pentenoyl]-4-(phenylmethyl)-1,3-oxazolidin-2-one (35)**. A mixture of **34** (3.29 g, 12.7 mmol), magnesium chloride (0.121 g, 1.27 mmol), NaSBF₆ (0.985 g, 3.81 mmol), triethylamine (3.54 mL, 25.4 mmol), *trans*-cinnamaldehyde (1.94 mL, 15.2 mmol), and TMSCl (2.43 mL, 19.0 mmol) in EtOAc (58 mL) was stirred at room temperature for 17 h. The mixture was diluted with EtOAc and filtered to remove solids. The filtrate was concentrated to small volume and then diluted with MeOH (50 mL) and a small amount of EtOAc. Following treatment with TFA (0.10 mL) the solution was stirred at room temperature for 1 h and then concentrated to dryness at reduced pressure. The residue was purified by flash chromatography (silica gel, 0–20% EtOAc/hexane) to give **35** (4.38 g, 88%) as a yellow semisolid. ¹H NMR (400 MHz, CDCl₃): δ 7.25–7.44 (m, 8 H), 7.13–7.20 (m, 2 H), 6.69 (d, *J* = 15.8 Hz, 1 H), 6.33 (dd, *J* = 15.9 Hz, 6.0 Hz, 1 H), 5.75–5.88 (m, 1 H), 5.12 (d, *J* = 17.2 Hz, 1 H), 5.05 (d, *J* = 10.2 Hz, 1 H), 4.63–4.76 (m, 1 H), 4.50–4.60 (m, 1 H), 4.25–4.35 (m, 1 H), 4.13–4.20 (m, 2 H), 3.25 (dd, *J* = 13.5 Hz, 3.3 Hz, 1 H), 2.82–3.00 (m, 1 H), 2.40–2.64 (m, 3 H). ES-LCMS *m/z*: 374 (M + 1 – H₂O).

(C) **(4*R*)-3-[(1*S*,2*S*)-2-Hydroxy-3-cyclopenten-1-yl]carbonyl]-4-(phenylmethyl)-1,3-oxazolidin-2-one (36)**. A solution of **35** (495 mg, 1.26 mmol) in toluene (60 mL) was degassed three times with nitrogen and treated with Grubbs third generation catalyst (65 mg, 0.089 mmol). The solution was degassed two more times with nitrogen and stirred at room temperature overnight. The solution was then concentrated to dryness at reduced pressure and the residue subjected to flash chromatography (silica gel, 0–40% EtOAc/hexane) to give **36** (340 mg, 94%) as a dark brown oil, which solidified upon

standing. ¹H NMR (400 MHz, CDCl₃): δ 7.25–7.40 (m, 3 H), 7.18–7.24 (m, 2 H), 6.00–6.08 (m, 1 H), 5.76–5.85 (m, 1 H), 5.00–5.08 (m, 1 H), 4.65–4.75 (m, 1 H), 4.20–4.35 (m, 2 H), 3.90–4.00 (m, 1 H), 3.29 (dd, *J* = 13.4 Hz, 3.2 Hz, 1 H), 2.90–3.15 (br s, 1 H), 2.75–2.90 (m, 3 H). ES-LCMS *m/z*: 270 (M + 1-H₂O).

(D) **(4*R*)-3-[(1*S*,2*S*,3*S*,5*S*)-2-Hydroxybicyclo[3.1.0]hex-3-yl]carbonyl]-4-(phenylmethyl)-1,3-oxazolidin-2-one**. A solution of **36** (330 mg, 1.15 mmol) in DCM (15 mL) was cooled in an ice bath and treated with 1 M diethylzinc in hexane (5.74 mL, 5.74 mmol) by dropwise addition. After the mixture was stirred at 0 °C for 20 min, diiodomethane (0.936 mL, 11.5 mmol) was added dropwise. The resulting cloudy solution was stirred at 0 °C for 20 min and then allowed to warm to room temperature. After 6 h, the reaction mixture was quenched with saturated aqueous ammonium chloride and extracted with EtOAc. The combined organic extracts were washed with brine, dried over sodium sulfate, and concentrated to dryness at reduced pressure. The crude material was purified by flash chromatography (silica gel, 0–40% EtOAc/hexane) to give the title compound (308 mg, 89%) as a light brown viscous oil. ¹H NMR (400 MHz, CDCl₃): δ 7.25–7.40 (m, 3 H), 7.20–7.24 (m, 2 H), 4.84–4.94 (m, 1 H), 4.64–4.74 (m, 1 H), 4.15–4.25 (m, 2 H), 3.57–3.66 (m, 1 H), 3.28 (dd, *J* = 13.5 Hz, 3.3 Hz, 1 H), 2.84 (dd, *J* = 13.4 Hz, 9.4 Hz, 1 H), 2.00–2.25 (m, 2 H), 1.60–1.70 (m, 1 H), 1.40–1.48 (m, 1 H), 0.65–0.73 (m, 1 H), 0.45–0.55 (m, 1 H). ES-LCMS *m/z*: 284 (M + 1 – H₂O).

(E) **(4*R*)-3-[(1*S*,2*S*,3*S*,5*S*)-2-[(1,1-Dimethylethyl)(dimethyl)silyloxy]bicyclo[3.1.0]hex-3-yl]carbonyl]-4-(phenylmethyl)-1,3-oxazolidin-2-one**. To a stirred solution of **(4*R*)-3-[(1*S*,2*S*,3*S*,5*S*)-2-hydroxybicyclo[3.1.0]hex-3-yl]carbonyl]-4-(phenylmethyl)-1,3-oxazolidin-2-one** (308 mg, 1.02 mmol) and 2,6-lutidine (0.475 mL, 4.09 mmol) in DCM (5 mL) at 0 °C was added TBSOTf (0.587 mL, 2.56 mmol) under nitrogen. The resulting mixture was stirred at 0 °C for 30 min, then room temperature for 1 h. Following addition of MeOH (0.30 mL), the mixture was poured into water and extracted with ether (2×). The combined ether extracts were washed with brine, dried over sodium sulfate, filtered, concentrated, and purified by flash chromatography (silica gel, 0–20% EtOAc/hexane) to give the title compound (406 mg, 96%) as a colorless oil. ¹H NMR (400 MHz, CDCl₃): δ 7.25–7.38 (m, 3 H), 7.17–7.22 (m, 2 H), 5.02–5.10 (m, 1 H), 4.63–4.73 (m, 1 H), 4.08–4.22 (m, 2 H), 3.57–3.66 (m, 1 H), 3.24 (dd, *J* = 13.4 Hz, 3.3 Hz, 1 H), 2.77 (dd, *J* = 13.4 Hz, 9.1 Hz, 1 H), 2.26 (dd, *J* = 11.9 Hz, 7.8 Hz, 1 H), 1.70–1.82 (m, 1 H), 1.42–1.50 (m, 1 H), 1.30–1.38 (m, 1 H), 0.90 (s, 9 H), 0.70–0.75 (m, 1 H), 0.40–0.47 (m, 1 H), 0.14 (s, 3 H), 0.08 (s, 3 H). ES-LCMS *m/z*: 416 (M + 1).

(F) **(1*S*,2*S*,3*S*,5*S*)-2-[(1,1-Dimethylethyl)(dimethyl)silyloxy]bicyclo[3.1.0]hexane-3-carboxylic Acid (37)**. To a solution of **(4*R*)-3-[(1*S*,2*S*,3*S*,5*S*)-2-[(1,1-dimethylethyl)(dimethyl)silyloxy]bicyclo[3.1.0]hex-3-yl]carbonyl]-4-(phenylmethyl)-1,3-oxazolidin-2-one** (405 mg, 0.974 mmol) in THF (6 mL) and water (2 mL) at 0 °C was added 30% aqueous hydrogen peroxide (0.796 mL, 7.80 mmol) dropwise, followed by addition of a solution of lithium hydroxide monohydrate (167 mg, 3.90 mmol) in water (1 mL). After being stirred for 1 h at 0 °C, the reaction mixture was stirred at room temperature overnight. The excess hydrogen peroxide was quenched by the addition of saturated aqueous sodium bisulfite (4 mL). The mixture was treated with 0.1 N NaOH (0.2 mL) and washed with ether (40 mL). The aqueous layer was acidified to pH 3 with 1 M aqueous potassium hydrogen sulfate and extracted with EtOAc (3 × 40 mL). The combined organic extracts were washed with brine, dried over sodium sulfate, filtered, and concentrated to give **37** (220 mg, 88%) as a colorless oil. ¹H NMR (400 MHz, CDCl₃): δ 4.65–4.75 (m, 1 H), 2.30–2.40 (m, 1 H), 1.96–2.10 (m, 2 H), 1.41–1.50 (m, 1 H), 1.32–1.40 (m, 1 H), 0.91 (s, 9 H), 0.56–0.62 (m, 1 H), 0.41–0.49 (m, 1 H), 0.13 (s, 3 H), 0.11 (s, 3 H).

(G) **(1*S*,2*S*,3*S*,5*S*)-2-[(1,1-Dimethylethyl)(dimethyl)silyloxy]bicyclo[3.1.0]hex-3-ylamine (38)**. To a solution of **37** (10.0 g, 39.0 mmol) in toluene (180 mL) were added TEA (6.52 mL, 46.8 mmol) and diphenylphosphoryl azide (8.43 mL, 39.0 mmol). The solution was heated to 80 °C for 5 h and then cooled to 0 °C in an ice bath. To this

solution was added potassium trimethylsilanolate (10.0 g, 78.0 mmol) in THF (90 mL) and the mixture stirred at room temperature for 1 h. The mixture was quenched by addition of 15% aqueous citric acid and then basified by addition of aqueous sodium hydroxide. The resulting mixture was extracted with ether. The ether layer was separated, and the aqueous layer was evaporated to a small volume and extracted again with ether. The combined ether solutions were washed with a small amount of saturated brine, dried over sodium sulfate, filtered, and evaporated to afford **38** (8.86 g, 95%) as a pale yellow oil, which was used without further purification. ¹H NMR (400 MHz, CDCl₃): δ 3.92–4.00 (m, 1 H), 2.60–2.70 (m, 1 H), 2.00–2.10 (m, 1 H), 1.50–1.60 (m, 1 H), 1.32–1.38 (m, 1 H), 1.20–1.29 (m, 1 H), 0.92 (s, 9 H), 0.56–0.60 (m, 1 H), 0.30–0.38 (m, 1 H), 0.12 (s, 3 H), 0.11 (s, 3 H).

(H) *N1-((1S,2S,3S,5S)-2-(((1,1-Dimethylethyl)(dimethyl)silyloxy)bicyclo[3.1.0]hex-3-yl)-N2-[(4-nitrophenyl)sulfonyl]glycinamide*. *N*-[(4-Nitrophenyl)sulfonyl]glycine (10.1 g, 39.0 mmol), **38** (8.86 g, 39.0 mmol), HOBT (6.56 g, 42.9 mmol), and DIPEA (8.17 mL, 46.8 mmol) were combined in DMF (187 mL). To this solution was added EDC (8.22 g, 42.9 mmol), and the reaction mixture was stirred at room temperature for 5 h. The mixture was diluted with EtOAc and poured into water. The organic layer was separated and washed with saturated aqueous sodium bicarbonate followed by brine. After drying over sodium sulfate, the solution was concentrated to dryness at reduced pressure. The resulting solid was triturated with ether, filtered, and dried to afford the title compound in quantitative yield, which was used without further purification. ES-LCMS *m/z*: 470 (M + 1).

(I) *1-((1S,2S,3S,5S)-2-(((1,1-Dimethylethyl)(dimethyl)silyloxy)bicyclo[3.1.0]hex-3-yl)-4-[(4-nitrophenyl)sulfonyl]-2-piperazinone*. *N1-((1S,2S,3S,5S)-2-(((1,1-Dimethylethyl)(dimethyl)silyloxy)bicyclo[3.1.0]hex-3-yl)-N2-[(4-nitrophenyl)sulfonyl]glycinamide* (18.3 g, 38.9 mmol), 1,2-dibromoethane (26.8 mL, 311 mmol), and cesium carbonate (50.7 g, 156 mmol) were combined in DMF (200 mL) and stirred at room temperature for 6 h. The mixture was diluted with EtOAc, washed with water, brine, dried over sodium sulfate, and concentrated to dryness at reduced pressure. The resulting solid was triturated with hexane/ether, filtered, and dried. The filtrate was concentrated at reduced pressure and the residue purified by flash chromatography (silica gel, EtOAc/hexane) to afford a solid, which when combined with the triturated solid, gave the title compound (15.8 g, 82%) as a yellow solid. ¹H NMR (400 MHz, CDCl₃): δ 8.42 (d, *J* = 8.8 Hz, 2 H), 7.99 (d, *J* = 8.5 Hz, 2 H), 4.62–4.70 (m, 1 H), 3.84–3.96 (m, 1 H), 3.79 (d, *J* = 16.3 Hz, 1 H), 3.69 (d, *J* = 16.4 Hz, 1 H), 3.37–3.44 (m, 3 H), 3.20–3.34 (m, 1 H), 1.90–2.00 (m, 1 H), 1.75–1.83 (m, 1 H), 1.32–1.40 (m, 1 H), 1.24–1.31 (m, 1 H), 0.83 (s, 9 H), 0.64–0.73 (m, 1 H), 0.38–0.48 (m, 1 H), 0.06 (s, 3 H), 0.00 (s, 3 H). ES-LCMS *m/z*: 496 (M + 1).

(J) *1-((1S,2S,3S,5S)-2-(((1,1-Dimethylethyl)(dimethyl)silyloxy)bicyclo[3.1.0]hex-3-yl)-2-piperazinone* (**39**). A solution of 1-((1S,2S,3S,5S)-2-(((1,1-dimethylethyl)(dimethyl)silyloxy)bicyclo[3.1.0]hex-3-yl)-4-[(4-nitrophenyl)sulfonyl]-2-piperazinone (15.6 g, 31.5 mmol) in MeCN (300 mL) was treated with thiophenol (9.72 mL, 94.0 mmol), followed by potassium carbonate (17.4 g, 126 mmol) at room temperature under nitrogen. The reaction mixture was stirred for 11 h, diluted with DCM (200 mL), filtered to remove solids, and concentrated to dryness at reduced pressure. The residue was purified by flash chromatography [silica gel, 0–5% MeOH (2 M in ammonia)/DCM] to give **39** (8.2 g, 84%) as a light-yellow oil. ¹H NMR (400 MHz, CDCl₃): δ 4.75 (dd, *J* = 8.0 Hz, 5.1 Hz, 1 H), 3.98 (dt, *J* = 10.7 Hz, 8.0 Hz, 1 H), 3.52 (s, 2 H), 3.25–3.31 (m, 2 H), 3.01–3.14 (m, 2 H), 2.07 (td, *J* = 11.6 Hz, 4.9 Hz, 2 H), 1.86 (dd, *J* = 12.3 Hz, 7.8 Hz, 1 H), 1.35–1.43 (m, 1 H), 1.26–1.33 (m, 1 H), 0.88 (s, 9 H), 0.71–0.77 (m, 1 H), 0.42 (td, *J* = 7.9 Hz, 5.8 Hz, 1 H), 0.09 (s, 3 H), 0.06 (s, 3 H).

(K) *4-[[3-Chloro-5-cyclopropyl-7-(trifluoromethyl)pyrazolo[1,5-*a*]pyridin-2-yl]carbonyl]-1-((1S,2S,3S,5S)-2-(((1,1-dimethylethyl)(dimethyl)silyloxy)bicyclo[3.1.0]hex-3-yl)-2-piperazinone*. DIPEA (13.8 mL, 79.0 mmol) was added to a mixture of **14** (8.45 g, 27.7 mmol) and **39** (8.20 g, 26.4 mmol) in THF (250 mL) at room temperature under nitrogen. The mixture was stirred for 30 min and then cooled to 0 °C. To the solution was added 50% T3P/EtOAc

(23.6 mL, 39.6 mmol). The mixture was allowed to warm to room temperature and stirred for 2 h. Saturated aqueous sodium bicarbonate was then added. The mixture was extracted with EtOAc (3×). The combined organic extracts were washed with brine, dried over sodium sulfate, and concentrated at reduced pressure to afford the title compound as a yellow oil in quantitative yield. This material was used in the next step without further purification. ES-LCMS *m/z*: 597 (M + 1).

(L) *4-[[3-Chloro-5-cyclopropyl-7-(trifluoromethyl)pyrazolo[1,5-*a*]pyridin-2-yl]carbonyl]-1-((1S,2S,3S,5S)-2-hydroxybicyclo[3.1.0]hex-3-yl)-2-piperazinone* (**28a**). TBAF (1 M in THF, 55.3 mL, 55.3 mmol) was added to a solution of 4-[[3-chloro-5-cyclopropyl-7-(trifluoromethyl)pyrazolo[1,5-*a*]pyridin-2-yl]carbonyl]-1-((1S,2S,3S,5S)-2-(((1,1-dimethylethyl)(dimethyl)silyloxy)bicyclo[3.1.0]hex-3-yl)-2-piperazinone (22.0 g, 36.8 mmol) in THF (350 mL) at 0 °C under nitrogen. The reaction mixture was allowed to warm to room temperature and stirred for 4 h. Most of the THF was removed at reduced pressure, and the residue was partitioned between EtOAc and saturated aqueous sodium bicarbonate. The phases were separated, and the aqueous solution was extracted with additional portions of EtOAc (3 × 100 mL). The combined EtOAc solutions were dried over sodium sulfate and concentrated to dryness at reduced pressure. The residue was purified by flash chromatography [silica gel, 20–90% EtOAc (containing 5% MeOH)/hexane] to give **28a** as a white foam (15.1 g, 85%). Mp 108–111 °C. ¹H NMR (400 MHz, CDCl₃): δ 7.38–7.47 (m, 1 H), 7.06 (br s, 1 H), 4.30–4.63 (m, 4 H), 4.15–4.22 (m, 1 H), 3.85–3.98 (m, 1 H), 3.40–3.54 (m, 2 H), 1.91–2.05 (m, 3 H), 1.53–1.64 (m, 1 H), 1.42 (br s, 1 H), 1.13–1.22 (m, 2 H), 0.84–0.90 (m, 2 H), 0.75–0.84 (m, 1 H), 0.46–0.58 (m, 1 H). HRMS *m/z* calcd for C₂₂H₂₂ClF₃N₄O₃ (M + 1): 483.1411. Found: 483.1414. LCMS purity: >98%. The enantiopurity was determined as >99% by chiral analytical HPLC [ChiralPak AD-H column (4.6 mm × 250 mm, 5 μm), isocratic at 70% EtOH/hexane]. The retention time was in agreement with that for **28a** obtained by preparative chiral SFC of the racemate (see Supporting Information) from the synthetic route shown in Scheme 4 (*t*_R of 5.9 and 3.5 min for **28a** and **28b**, respectively). Specific rotation [*α*] was +40°, measured at 589 nm and 25 °C. A 50 mg portion of the product was crystallized as follows. The material was slurried in ethyl ether and the mixture sonicated until the solid had dissolved. The solution was seeded with a trace of crystalline **28a** and the mixture stirred while the ether was allowed to slowly evaporate to dryness. The resulting solid was dried under vacuum. Mp 134–137 °C. The material was determined to be crystalline by both polarized light microscopy and PXRD analysis.

■ ASSOCIATED CONTENT

📄 Supporting Information

Experimental details for the syntheses and spectroscopic characterization of the compounds in this paper. This material is available free of charge via the Internet at <http://pubs.acs.org>. The X-ray crystal structure of compound (+)-**28a** has been deposited at the Cambridge Crystallographic Data Centre (disposition number CCDC 900754).

■ AUTHOR INFORMATION

Corresponding Author

*E-mail: andy.j.peat@gsk.com. Phone: 919-483-6137.

Present Addresses

[†]For M.Y.: Lieber Institute for Brain Development, 855 N. Wolfe Street, Baltimore, MD 21205, U.S.

[‡]For A.M.: Salix Pharmaceuticals, Inc., 8510 Colonnade Drive, Raleigh, NC 27615, U.S.

Notes

The authors declare the following competing financial interest(s): All of the authors are/were employees of GlaxoSmithKline where this work was completed.

ACKNOWLEDGMENTS

The authors acknowledge the contributions of the following GSK scientists to the manuscript: Todd Baughman (reactive metabolite data), George Dorsey (NMR structure elucidation), Douglas Minnick (vibrational circular dichroism spectroscopy), Iris Paulus (chromatographic log *D* measurements and high resolution mass spectrometry), Eric Wentz and Yang Zhao (chromatographic purification), Greg Robertson and Tucker Sheppard (solubility measurements).

ABBREVIATIONS USED

AcOH, acetic acid; (Bpin)₂, bis(pinacolato)diboron; BEI, binding efficiency index ($=(\text{pIC}_{50}/\text{MW}) \times 1000$); Chrom-LogD, chromatographically measured log *D*; Cl, clearance; DAA, direct acting antiviral; DIPEA, *N,N*-diisopropylethylamine; DMAD, dimethylacetylene dicarboxylate; DPPA, diphenylphosphorylazide; EDC, *N*-ethyl-*N'*-(3-dimethylaminopropyl)carbodiimide hydrochloride; EtOAc, ethyl acetate; HAART, highly active antiretroviral therapy; HOBt, *N*-hydroxybenzotriazole; HP- β -CD, 2-hydroxypropyl- β -cyclodextrin; IFN, pegylated interferon; KOTMS, potassium trimethylsilanoate; LLE, lipophilic ligand efficiency; $\text{LLE}_{\text{calc}} = \text{pIC}_{50} - \text{cLogP}$; $\text{LLE}_{\text{meas}} = \text{pIC}_{50(\text{NS4B Binding})} - \text{ChromLogD}$; MeCN, acetonitrile; MeOH, methanol; MSH, *O*-mesitylensulfonylhydroxylamine; NS, nonstructural; Ns, 4-nitrophenylsulfonyl; NS4B, nonstructural protein 4B; PXRD, powder X-ray diffraction; SFC, supercritical fluid chromatography; SoC, standard of care; T3P, 1-propanephosphonic anhydride; TBSOTf, trimethylsilyl trifluoromethanesulfonate; TEA, triethylamine; TFA, trifluoroacetic acid; TMSCl, trimethylsilyl chloride

REFERENCES

- (1) Te, H. S.; Jensen, D. M. Epidemiology of Hepatitis B and C Viruses: A Global Overview. *Clin. Liver Dis.* **2010**, *14*, 1–21.
- (2) Shepard, C. W.; Finelli, L.; Alter, M. J. Global Epidemiology of Hepatitis C Virus Infection. *Lancet Infect. Dis.* **2005**, *5*, 558–567.
- (3) El-Serag, H. B. Epidemiology of Viral Hepatitis and Hepatocellular Carcinoma. *Gastroenterology* **2012**, *142*, 1264–1273.
- (4) Perz, J. F.; Armstrong, G. L.; Farrington, L. A.; Hutin, Y. J. F.; Bell, B. P. The Contributions of Hepatitis B Virus and Hepatitis C Virus Infections to Cirrhosis and Primary Liver Cancer Worldwide. *J. Hepatol.* **2006**, *45*, 529–538.
- (5) Yeh, W.-S.; Armstrong, E. P.; Skrepnek, G. H.; Malone, D. C. Peginterferon Alfa-2a versus Peginterferon Alfa-2b as Initial Treatment of Hepatitis C Virus Infection: a Cost-Utility Analysis from the Perspective of the Veterans Affairs Health Care System. *Pharmacotherapy* **2007**, *27*, 813–824.
- (6) Kwong, A. D.; Kauffman, R. S.; Hurter, P.; Mueller, P. Discovery and Development of Telaprevir: An NS3-4A Protease Inhibitor for Treating Genotype 1 Chronic Hepatitis C Virus. *Nat. Biotechnol.* **2011**, *29*, 993–1003.
- (7) Venkatraman, S. Discovery of Boceprevir, a Direct-Acting NS3/4A Protease Inhibitor for Treatment of Chronic Hepatitis C Infections. *Trends Pharmacol. Sci.* **2012**, *33*, 289–294.
- (8) Chen, K. X.; Njoroge, F. G. The Journey to the Discovery of Boceprevir: An NS3-NS4 HCV Protease Inhibitor for the Treatment of Chronic Hepatitis C. *Prog. Med. Chem.* **2010**, *49*, 1–36.
- (9) Russo, M. W.; Fried, M. W. Side Effects of Therapy for Chronic Hepatitis C. *Gastroenterology* **2003**, *124*, 1711–1719.
- (10) Manns, M. P.; Wedemeyer, H.; Cornberg, M. Treating Viral Hepatitis C: Efficacy, Side Effects, and Complications. *Gut* **2006**, *55*, 1350–1359.

(11) Asselah, T.; Marcellin, P. Direct Acting Antivirals for the Treatment of Chronic Hepatitis C: One Pill a Day for Tomorrow. *Liver Int.* **2012**, *32* (Suppl. 1), 88–102.

(12) Welsch, C.; Jesudian, A.; Zeuzem, S.; Jacobson, I. New Direct-Acting Antiviral Agents for the Treatment of Hepatitis C Virus Infection and Perspectives. *Gut* **2012**, *61*, i36–i46.

(13) Pockros, P. J. Drugs in Development for Chronic Hepatitis C: a Promising Future. *Expert Opin. Biol. Ther.* **2011**, *11*, 1611–1622.

(14) Fusco, D. N.; Chung, R. T. Novel Therapies for Hepatitis C: Insights from the Structure of the Virus. *Annu. Rev. Med.* **2012**, *63*, 373–387.

(15) Lemon, S. M.; McKeating, J. A.; Pietschmann, T.; Frick, D. N.; Glenn, J. S.; Tellinghuisen, T. L.; Symons, J.; Furman, P. A. Development of Novel Therapies for Hepatitis C. *Antiviral Res.* **2010**, *86*, 79–92.

(16) Rice, C. M.; Kolykhalov, A. A.; Lin, C.; Reed, K.; Agapov, E. A.; Blight, K.; Xu, J.; Grakoui, A. Virus Hepatitis C Virus Genome Organization and Expression: Potential Antiviral Targets. *Antiviral Ther.* **1996**, *1*, 11–17.

(17) Xiong, Y.-L.; Zhang, C.-J.; Wang, X.-H. Hepatitis C Virus Genomic Structure and Function. *Zhongguo Shengwu Huaxue Yu Fenzi Shengwu Xuebao* **2008**, *24*, 587–592.

(18) Belzhelarskaya, S. N.; Koroleva, N. N.; Popenko, V. V.; Druzha, V. L.; Orlova, O. V.; Rubtsov, P. M.; Kochetkov, S. N. Hepatitis C Virus Structural Proteins and Virus-like Particles Produced in Recombinant Baculovirus-Infected Insect Cells. *Mol. Biol. (Moscow, Russ. Fed., Engl. Ed.)* **2010**, *44*, 97–108.

(19) Beaulieu, P. L.; Llinas-Brunet, M. Therapies for Hepatitis C Infection: Targeting the Non-Structural Proteins of HCV. *Curr. Med. Chem.: Anti-Infect. Agents* **2002**, *1*, 163–176.

(20) Mani, N.; Rao, B. G.; Kieffer, T. L.; Kwong, A. D. Recent Progress in the Development of HCV Protease Inhibitors. *Methods Princ. Med. Chem.* **2011**, *50*, 307–328.

(21) Chary, A.; Holodniy, M. Recent Advances in Hepatitis C Virus Treatment: Review of HCV Protease Inhibitor Clinical Trials. *Rev. Recent Clin. Trials* **2010**, *5*, 158–173.

(22) Kwo, P. Y.; Vinayek, R. The Therapeutic Approaches for Hepatitis C Virus: Protease Inhibitors and Polymerase Inhibitors. *Gut Liver* **2011**, *5*, 406–417.

(23) Li, H.; Shi, S. T. Non-Nucleoside Inhibitors of Hepatitis C Virus Polymerase: Current Progress and Future Challenges. *Future Med. Chem.* **2010**, *2*, 121–141.

(24) Sofia, M. J.; Chang, W.; Furman, P. A.; Mosley, R. T.; Ross, B. S. Nucleoside, Nucleotide, and Non-Nucleoside Inhibitors of Hepatitis C Virus NSSB RNA-Dependent RNA-Polymerase. *J. Med. Chem.* **2012**, *55*, 2481–2531.

(25) Reviriego, C. Daclatasvir Dihydrochloride: Treatment of Hepatitis C Virus HCV NSSA Inhibitor. *Drugs Future* **2011**, *36*, 735–739.

(26) Este, J. A.; Cihlar, T. Current Status and Challenges of Antiretroviral Research and Therapy. *Antiviral Res.* **2010**, *85*, 25–33.

(27) De Clercq, E. The Design of Drugs for HIV and HCV. *Nat. Rev. Drug Discovery* **2007**, *6*, 1001–1018.

(28) Gane, E. J.; Stedman, C. A.; Hyland, R. H.; Phil, D.; Ding, X.; Svarovskaia, E.; Symonds, W. T.; Hinds, R. G.; Berrey, M. M. Nucleotide Polymerase Inhibitor Sofosbuvir plus Ribavirin for Hepatitis C. *N. Engl. J. Med.* **2013**, *368*, 34–44.

(29) Stedman, C. A. M. Current Prospects for Interferon-Free Treatment of Hepatitis C in 2012. *J. Gastroenterol. Hepatol.* **2013**, *28*, 38–45.

(30) Rong, L.; Dahari, H.; Ribeiro, R. M.; Perelson, A. S. Rapid Emergence of Protease Inhibitor Resistance in Hepatitis C Virus. *Sci. Transl. Med.* **2010**, *2*, 1–9.

(31) Shotwell, J. B.; Baskaran, S.; Chong, P.; Creech, K. L.; Crosby, R. M.; Dickson, H.; Fang, J.; Garrido, D.; Mathis, A.; Maung, J.; Parks, D. J.; Pouliot, J. J.; Price, D. J.; Rai, R.; Seal, J. W.; Schmitz, U.; Tai, V. W. F.; Thomson, M.; Xie, M.; Xiong, Z. Z.; Peat, A. J. Imidazo[1,2-*a*]pyridines That Directly Interact with Hepatitis C NS4B: Initial Preclinical Characterization. *ACS Med. Chem. Lett.* **2012**, *3*, 565–569.

- (32) Banka, A.; Catalano, J. G.; Chong, P. Y.; Fang, J.; Garrido, D. M.; Peat, A. J.; Price, D. J.; Shotwell, J. B.; Tai, V.; Zhang, H. Preparation of Piperazinyl Antiviral Agents. WO2011041713A2, April 7, 2011.
- (33) Banka, A.; Catalano, J. G.; Chong, P. Y.; Fang, J.; Garrido, D. M.; Maynard, A.; Miller, J.; Patterson, D.; Peat, A. J.; Powers, J.; Price, D. J.; Roberts, C.; Tai, V.; Youngman, M. Preparation of 1-Piperidinyl- and 1-Piperazinylpyrazolo[1,5-*a*]pyridin-2-ylmethanone Derivatives as Antiviral Agents. WO2011050284A1, April 28, 2011.
- (34) Rai, R.; Deval, J. New Opportunities in Anti-Hepatitis C Virus Drug Discovery: Targeting NS4B. *Antiviral Res.* **2011**, *90*, 93–101.
- (35) Gouttenoire, J.; Penin, F.; Moradpour, D. Hepatitis C Virus Nonstructural Protein 4B: A Journey into Unexplored Territory. *Rev. Med. Virol.* **2010**, *20*, 117–129.
- (36) Cho, N.-J.; Dvory-Sobol, H.; Lee, C.; Cho, S.-J.; Bryson, P.; Masek, M.; Elazar, M.; Frank, C. W.; Glenn, J. S. Identification of a Class of HCV Inhibitors Directed against the Nonstructural Protein NS4B. *Sci. Transl. Med.* **2010**, *2*, 1–8.
- (37) Dvory-Sobol, H.; Pang, P. S.; Glenn, J. S. The Future of HCV Therapy: NS4B as an Antiviral Target. *Viruses* **2010**, *2*, 2481–2492.
- (38) Meuleman, P.; Leroux-Roels, G. HCV Animal Models: A Journey of More Than 30 Years. *Viruses* **2009**, *1*, 222–240.
- (39) Olsen, D. B.; Davies, M.-E.; Handt, L.; Koeplinger, K.; Zhang, N. R.; Ludmerer, S. W.; Graham, D.; Liverton, N.; MacCoss, M.; Hazuda, D.; Carroll, S. S. Sustained Viral Response in a Hepatitis C Virus-Infected Chimpanzee via a Combination of Direct-Acting Antiviral Agents. *Antimicrob. Agents Chemother.* **2011**, *55*, 937–939.
- (40) Kikuchi, R.; McCown, M.; Olson, P.; Tateno, C.; Morikawa, Y.; Katoh, Y.; Bourdet, D. L.; Monshouer, M.; Fretland, A. J. Effect of Hepatitis C Virus Infection on the mRNA Expression of Drug Transporters and Cytochrome p450 Enzymes in Chimeric Mice with Humanized Liver. *Drug Metab. Dispos.* **2010**, *38*, 1954–1961.
- (41) Kneteman, N. M.; Howe, A. Y. M.; Gao, T.; Lewis, J.; Pevear, D.; Lund, G.; Douglas, D.; Mercer, D. F.; Tyrrell, D. L. J.; Immermann, F.; Chaudhary, I.; Speth, J.; Villano, S. A.; O'Connell, J.; Collett, M. HCV796: A Selective Nonstructural Protein 5B Polymerase Inhibitor with Potent Anti-Hepatitis C Virus Activity in Vitro, in Mice with Chimeric Human Livers, and in Humans Infected with Hepatitis C Virus. *Hepatology* **2009**, *49*, 745–752.
- (42) Pouliot, J. J.; Thomson, M.; Xie, M.; Horton, J.; Johnson, J.; Krull, D.; Mathis, A.; Morikawa, Y.; Parks, D.; Peterson, R.; Shimada, T.; Thomas, E.; Vamathevan, J.; Van Horn, S.; Xiong, Z.; Hamatake, R.; Peat, A. J. Unpublished results.
- (43) Roberts, C. D.; Peat, A. J. HCV Replication Inhibitors That Interact with NS4B. In *Successful Strategies for the Discovery of Antiviral Drugs*; Meanwell, N., Desai, M. C., Eds.; Royal Society of Chemistry; Cambridge, U.K., 2013; Chapter 6.
- (44) Carpino, L. A. *O*-Acyloxyhydroxylamines. II. *O*-Mesitylenesulfonyl-, *O*-(*p*-Toluenesulfonyl)-, and *O*-Mesitylthiohydroxylamine. *J. Am. Chem. Soc.* **1960**, *82*, 3133–3135.
- (45) Tamura, Y.; Minamikawa, J.; Miki, Y.; Matsugashita, S.; Ikeda, M. A Novel Method for Heteroaromatic *N*-Imines. *Tetrahedron Lett.* **1972**, *13*, 4133–4135.
- (46) Other *N*-aminating reagents, hydroxylamine-*O*-sulfonic acid and *O*-(2,4-dinitrophenyl)hydroxylamine, failed to effect the desired transformation.
- (47) Anderson, P. L.; Hasak, J. P.; Kahle, A. D.; Paoletta, N. A.; Shapiro, M. J. 1,3-Dipolar Addition of Pyridine *N*-Imine to Acetylenes and the Use of Carbon-13 NMR in Several Structural Assignments. *J. Heterocycl. Chem.* **1981**, *18*, 1149–1152.
- (48) Kendall, J. D. Synthesis and Reactions of Pyrazolo[1,5-*a*]pyridines and Related Heterocycles. *Curr. Org. Chem.* **2011**, *15*, 2481–2518.
- (49) Loeber, S.; Huebner, H.; Utz, W.; Gmeiner, P. Rationally Based Efficacy Tuning of Selective Dopamine D4 Receptor Ligands Leading to the Complete Antagonist 2-[4-(4-Chlorophenyl)piperazin-1-ylmethyl]pyrazolo[1,5-*a*]pyridine (FAUC 213). *J. Med. Chem.* **2001**, *44*, 2691–2694.
- (50) Although MSH has been prepared and safely used on kilogram scale, its instability prevents safe storage (see ref 51).
- (51) Mendiola, J.; Rincon, J. A.; Mateos, C.; Soriano, J. F.; de, F.; Niemeier, J. K.; Davis, E. M. Preparation, Use, and Safety of *O*-Mesitylenesulfonylhydroxylamine. *Org. Process Res. Dev.* **2009**, *13*, 263–267.
- (52) Wunderlich, S. H.; Knochel, P. (tmp)₂Zn–2MgCl₂–2 LiCl: A Chemoselective Base for the Directed Zincation of Sensitive Arenes and Heteroarenes. *Angew. Chem., Int. Ed.* **2007**, *46*, 7685–7688.
- (53) Dong, Z.; Clososki, G. C.; Wunderlich, S. H.; Unsinn, A.; Li, J.; Knochel, P. Direct Zincation of Functionalized Aromatics and Heterocycles by Using a Magnesium Base in the Presence of ZnCl₂. *Chem.—Eur. J.* **2009**, *15*, 457–468.
- (54) Chen, Q.; Wu, S. Methyl (Fluorosulfonyl)difluoroacetate; a New Trifluoromethylating Agent. *J. Chem. Soc., Chem. Commun.* **1989**, 705–706.
- (55) Roy, S.; Gregg, B. T.; Gribble, G. W.; Le, V.-D.; Roy, S. Trifluoromethylation of Aryl and Heteroaryl Halides. *Tetrahedron* **2011**, *67*, 2161–2195.
- (56) Bullock, K.; Chong, P.; Davis, R.; Elitzin, V.; Hatcher, M.; Jackson, M.; Liu, B.; Patterson, D.; Powers, J.; Salmons, M.; Tabet, E.; Toczko, M. Ir C–H Activation and Other Catalysis Applied to a Complex Drug Candidate. *Top. Catal.* **2012**, *55*, 446–452.
- (57) Chong, P.; Davis, R.; Elitzin, V.; Hatcher, M.; Liu, B.; Salmons, M.; Tabet, E. Synthesis of 7-Trifluoromethylpyrazolo[1,5-*a*]pyridinedicarboxylate. *Tetrahedron Lett.* **2012**, *53*, 6786–6788.
- (58) Ishiyama, T.; Takagi, J.; Ishida, K.; Miyaura, N.; Anastasi, N. R.; Hartwig, J. F. Mild Iridium-Catalyzed Borylation of Arenes. High Turnover Numbers, Room Temperature Reactions, and Isolation of a Potential Intermediate. *J. Am. Chem. Soc.* **2002**, *124*, 390–391.
- (59) Ishiyama, T.; Nobuta, Y.; Hartwig, J. F.; Miyaura, N. Room Temperature Borylation of Arenes and Heteroarenes Using Stoichiometric Amounts of Pinacolborane Catalyzed by Iridium Complexes in an Inert Solvent. *Chem. Commun. (Cambridge, U. K.)* **2003**, 2924–2925.
- (60) Hartwig, J. F. Borylation and Silylation of C–H Bonds: A Platform for Diverse C–H Bond Functionalizations. *Acc. Chem. Res.* **2012**, *45*, 864–873.
- (61) Leeson, P. D.; Empfield, J. R. Reducing the Risk of Drug Attrition Associated with Physicochemical Properties. *Annu. Rep. Med. Chem.* **2010**, *45*, 393–407.
- (62) Hann, M. M.; Keserue, G. M. Finding the Sweet Spot: The Role of Nature and Nurture in Medicinal Chemistry. *Nat. Rev. Drug Discovery* **2012**, *11*, 355–365.
- (63) Meanwell, N. A. Improving Drug Candidates by Design: A Focus on Physicochemical Properties as a Means of Improving Compound Disposition and Safety. *Chem. Res. Toxicol.* **2011**, *24*, 1420–1456.
- (64) Leeson, P. D.; Springthorpe, B. The Influence of Drug-like Concepts on Decision-Making in Medicinal Chemistry. *Nat. Rev. Drug Discovery* **2007**, *6*, 881–890.
- (65) Young, R. J.; Green, D. V. S.; Luscombe, C. N.; Hill, A. P. Getting Physical in Drug Discovery II: The Impact of Chromatographic Hydrophobicity Measurements and Aromaticity. *Drug Discovery Today* **2011**, *16*, 822–830.
- (66) ACD/logD; Advanced Chemistry Development, Inc.: Toronto, Ontario, Canada, 2012.
- (67) The bicyclo[3.1.0]hexan-6-ol was observed to undergo ring-opening to the aldehyde.
- (68) Trachtenberg, E. N.; Carver, J. R. Stereochemistry of Selenium Dioxide Oxidation of Cyclohexenyl Systems. *J. Org. Chem.* **1970**, *35*, 1646–1653.
- (69) Charette, A. B.; Beauchemin, A. Simmons–Smith cyclopropanation reaction. *Org. React.* **2004**, 1–415.
- (70) Friedrich, E. C.; Biresaw, G. Zinc Dust-Cuprous Chloride Promoted Cyclopropanations of Allylic Alcohols Using Ethylidene Iodide. *J. Org. Chem.* **1982**, *47*, 1615–1618.
- (71) Evans, D. A.; Tedrow, J. S.; Shaw, J. T.; Downey, C. W. Diastereoselective Magnesium Halide-Catalyzed anti-Aldol Reactions

of Chiral *N*-Acylloxazolidinones. *J. Am. Chem. Soc.* **2002**, *124*, 392–393.

(72) Ma, B.; Lee, W.-C. A Modified Curtius Reaction: An Efficient and Simple Method for Direct Isolation of Free Amine. *Tetrahedron Lett.* **2010**, *51*, 385–386.

(73) Fukuyama, T.; Jow, C.-K.; Cheung, M. 2- and 4-Nitrobenzenesulfonamides: Exceptionally Versatile Means for Preparation of Secondary Amines and Protection of Amines. *Tetrahedron Lett.* **1995**, *36*, 6373–6374.

(74) Obach, R. S.; Baxter, J. G.; Liston, T. E.; Silber, B. M.; Jones, B. C.; Macintyre, F.; Rance, D. J.; Wastall, P. The Prediction of Human Pharmacokinetic Parameters from Preclinical and in Vitro Metabolism Data. *J. Pharmacol. Exp. Ther.* **1997**, *283*, 46–58.

(75) Jacobson, L.; Middleton, B.; Holmgren, J.; Eirefelt, S.; Froejd, M.; Blomgren, A.; Gustavsson, L. An Optimized Automated Assay for Determination of Metabolic Stability Using Hepatocytes: Assay Validation, Variance Component Analysis, and in Vivo Relevance. *Assay Drug Dev. Technol.* **2007**, *5*, 403–415.